Biomaterials Science

ROYAL SOCIETY OF CHEMISTRY

REVIEW

View Article Online
View Journal | View Issue

Cite this: *Biomater. Sci.*, 2026, **14**, 2824

Thermoresponsive hydrogels for controlled drug delivery to the back of the eye: a data-driven guide to formulation design

Alexa K. Beathard-Wojan and Vibhuti Agrahari *

Hydrogels are water-rich, biocompatible three-dimensional polymer networks widely recognized for their ability to control drug release at specific target sites. Among them, *in situ* forming thermoresponsive hydrogels have emerged as promising injectable platforms for long-acting drug delivery to the posterior segment of the eye. These systems can reduce injection frequency, improve patient adherence, and minimize complications associated with repeated intravitreal dosing. However, the absence of standardized formulation and evaluation methodologies limits clinical translation. This study provides a comprehensive overview of drug-loaded, thermoresponsive hydrogels designed for intravitreal administration. It examines the influence of polymer composition and therapeutic class on key hydrogel properties, including mechanical behavior, safety, and drug-release performance, based on qualitative and quantitative analyses of 35 preclinical studies. Special attention is given to systems achieving prolonged drug release while maintaining biodegradability and biocompatibility. The findings consolidate current evidence and offer guidance for rational formulation design, highlighting how polymer structure and physicochemical characteristics can be tuned to optimize sustained ocular drug delivery and advance translation toward long-acting treatment of posterior segment diseases.

Received 23rd January 2026,
Accepted 23rd March 2026

DOI: 10.1039/d6bm00104a

rsc.li/biomaterials-science

Introduction

Vision impairment affects approximately 2.2 billion individuals worldwide, significantly limiting functional activities such as mobility and reading, fostering social isolation, and imposing a substantial economic burden on healthcare systems. Globally, productivity losses associated with vision impairment are estimated at $411 billion annually, primarily due to reduced workforce participation and performance. Of the five leading causes of vision impairment, three involve the posterior segment of the eye.[1] Despite the fact that more than half of all vision-impairing ocular diseases affect the posterior segment, few therapeutic modalities are designed to effectively target this region.[2] Of particular relevance to the present work are diabetic retinopathy (DR) and age-related macular degeneration (AMD), which serve as the primary focus of this review. In the United States, DR remains the leading cause of blindness among adults, while AMD is the predominant cause of irreversible central vision loss in individuals over 65 years of age.[3]

Topical administration routes have been extensively explored; however, less than 1% of applied drug reaches the posterior segment, resulting in limited clinical efficacy.[4] Periocular injections have been investigated as an alternative approach, wherein compounds are administered outside the globe of the eye and diffuse through the sclera, choroid, and retinal pigment epithelium (RPE). While this route is less invasive and poses fewer risks than intravitreal injection, its use for retinal treatment remains limited due to additional diffusion barriers.[2] Consequently, intravitreal injection or implantation offers the highest drug bioavailability at the retina and macula owing to direct access to the vitreous cavity. Yet, these procedures are associated with significant drawbacks, including discomfort, cost, and elevated risks of hemorrhage, retinal detachment, photoreceptor degeneration, cataract formation, bacterial endophthalmitis, and elevated intraocular pressure.[4] For chronic conditions, like AMD and DR, the cumulative burden of repeated injections imposes significant physical, financial, and safety challenges, underscoring the need for innovative, long-acting delivery systems capable of sustaining therapeutic concentrations over extended durations.[5]

Hydrogels represent a promising alternative for intravitreal drug delivery due to their capacity to extend drug release duration while reducing injection frequency. Broadly defined as three-dimensional, water-swollen polymer networks, hydrogels

Department of Pharmaceutical Sciences, University of Oklahoma Health Campus, 1110 N Stonewall Ave, Oklahoma City, Oklahoma, USA.
E-mail: Vibhuti-Agrahari@ou.edu

are distinguished by their biocompatibility, biodegradability, and tunable drug-release properties.[6,7] In ocular applications, hydrogels offer several advantages: their viscoelastic nature mimics the vitreous humor, they can encapsulate both small and large molecule therapeutics, and they can protect sensitive biomolecules from enzymatic degradation and clearance, thereby enhancing intraocular bioavailability. In addition, hydrogels can be designed to co-deliver multiple agents, enabling simplified treatment regimens for complex diseases. Of particular relevance are stimuli-responsive hydrogels, which undergo sol–to-gel transitions in response to environmental triggers such as pH, temperature, or light, allowing for injectable formulations that overcome the need for surgical implantation.[8,9]

Preclinical investigations of intravitreal hydrogels for drug delivery have been widely reported, encompassing both small molecules and biologics in diverse polymeric formulations for diseases such as glaucoma, wet AMD, and retinal neovascularization.[10,11] Despite promising outcomes *in vitro* and *in vivo*, few hydrogel-based systems have progressed into clinical development. To date, there is only one intraocular hydrogel system OTX-TKI, a PEG-based hydrogel fiber embedding tyrosine kinase inhibitor (TKI) microcrystals, that has progressed to phase 3 clinical trials in patients with wet AMD.[12,13]

Existing studies utilize diverse polymer types, formulation techniques, and evaluation methodologies which makes direct comparisons between different research groups difficult and slows translational progress. The present review addresses this gap by compiling and analyzing data from published reports of thermoresponsive hydrogels designed for intravitreal drug delivery. Specifically, this study identifies the relationships between hydrogel composition and resulting characteristics including swelling ratio, pore size, biodegradability, and drug release kinetics in relation to polymer origin and therapeutic class. Collectively, these findings provide a consolidated overview of current research and highlight key design parameters to guide the rational development of long-acting, thermoresponsive hydrogel platforms for sustained delivery to the posterior segment.

Posterior ocular anatomy and barriers relevant to drug delivery

The eye is anatomically divided into anterior and posterior segments. The posterior segment contains the sclera, choroid vessels, retina, macula, optic nerve, Bruch's membrane, RPE, and vitreous humor.[14] Each component of the eye has unique barriers to penetration, but for retinal delivery by intravitreal injection, compounds must permeate through the vitreous humor and into the retinal layers.[4,14]

The vitreous humor is approximately 98% water but also contains structural components such as collagen and hyaluronic acid (HA). The formed vitreous network has a large mesh size (~500 nm) and thus diffusion across the vitreous should not be limited by size aside from very large molecules. However, due to the negative charge of HA, positively charged molecules may bind within the vitreous, thereby limiting diffusion.[4,15] Once a compound reaches the retina, it must traverse several layers, with the inner limiting membrane (ILM) serving as the primary barrier in direct contact with the vitreous. Since the ILM is too fragile to be isolated, the exact permeability is difficult to determine *ex vivo* but is generally estimated to have pore sizes ranging from 10–25 nm.[15,16] Nonetheless, successful penetration of larger molecules (up to ~300 nm) has been demonstrated, indicating that molecular size alone does not dictate permeability.[16,17] The ILM, like the vitreous, is rich in negatively charged glycosaminoglycans, further limiting the diffusion of cationic compounds.[2,15] Given the negatively charged components of both the vitreous and ILM, charge is the largest barrier to transport of compounds after intravitreal injection (Fig. 1).

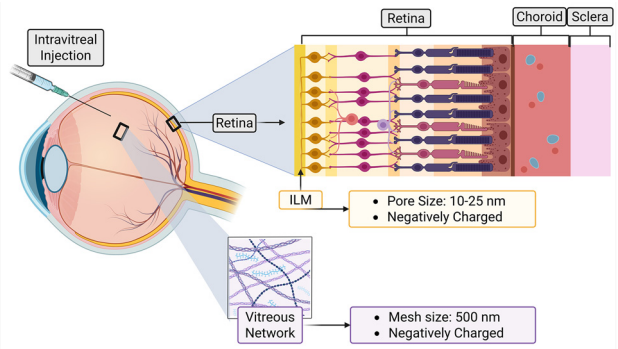

Fig. 1 Biological barriers to retinal delivery of therapeutics following intravitreal administration. Created in BioRender. Beathard, A. (2025). https://BioRender.com/34901w3.

Types of hydrogels used for intraocular delivery

Hydrogels can be classified based on the polymer origin, physical or mechanical properties, ionic charge, preparation procedure, or their responsiveness to external stimuli. Numerous comprehensive reviews describe these classifications in detail.[6,7,10,18] Therefore, this discussion focuses on hydrogel classes most relevant to intravitreal drug delivery applications.

Polymer origin

Hydrogels can be formulated using either natural or synthetic polymers, each offering distinct advantages and limitations. Natural polymers such as collagen, hyaluronan, and chitosan are typically non-toxic, biodegradable, cost-effective, readily available, and possess intrinsic bioactivity, including the ability to interact with biological proteins and facilitate cell penetration. However, hydrogels derived from natural polymers often exhibit reduced mechanical strength, lower stability, and faster degradation rates compared to their synthetic counterparts. In contrast, synthetic polymers such as polyethylene glycol (PEG), polyvinyl alcohol (PVA), and poloxamers offer greater mechanical strength, chemical stability, and customizable degradation profiles, but often require greater biocompatibility testing and formulation optimization to ensure safety in biomedical applications. To leverage the

strengths of both classes, hybrid hydrogels are often developed, combining the biological functionality of natural polymers with the structural integrity and customizability of synthetic ones.[7,10,19,20]

Stimuli responsiveness

Hydrogels can be engineered to undergo structural or phase transitions in response to external stimuli such as pH, temperature, ion concentration, light exposure, and electric or magnetic fields. Although ion- and pH-responsive hydrogels have been explored, they require extensive optimization and safety validation to minimize the risk of ocular irritation.[21] Consequently, temperature-sensitive systems are the most commonly employed in the ocular space. Lower critical solution temperature (LCST)-responsive hydrogels remain in a liquid state at room temperature and gel at physiological temperatures, effectively addressing challenges related to injectability associated with preformed gels.[22] This sol-to-gel transition arises from the self-assembly of amphiphilic copolymers, which reorganize from dispersed unimers into interconnected polymeric networks, forming a semi-solid matrix within the vitreous cavity.[22–25]

Key physicochemical and biological properties

Viscosity and rheological behavior. Viscosity and rheological properties characterize the flow behavior and deformability of hydrogels, encompassing parameters such as shear stress, the force required to disrupt structural order, and strain, which quantifies deformation. Elastic materials return to their original shape upon removal of force, with elasticity describing the extent of reversible deformation. In contrast, viscous materials continuously deform under applied force, and viscosity quantifies the rate of flow.[26] Hydrogels exhibit both elastic and viscous behavior and are thus classified as viscoelastic materials. Their viscoelasticity allows them to withstand the mechanical stress caused by fluid flow within the vitreous; therefore, limiting tissue damage at the site of implantation and ensuring the hydrogel structure can be maintained in the intended environment.[7,27]

Swelling ratio and water content. A defining property of hydrogels is their capacity to swell in aqueous environments. Owing to their high water content, which closely resembles that of human tissues, hydrogels are often biocompatible and offer potential for drug delivery applications due to the ability to transport diverse materials such as cells, proteins, and hydrophilic compounds.[27] The degree of swelling is governed by interactions between polymer chains and water molecules, as well as the elasticity of the hydrogel network. Initially, swelling is controlled by the rate that water can diffuse into the hydrogel, after which swelling is controlled by the rate that the polymer chains relax. The extent of swelling at equilibrium is characterized by the balance of multiple forces: polymer–water interactions, elastic retractive forces from stretched polymer chains, and osmotic forces arising from ionic species within or surrounding the hydrogel.[28] Crosslink density plays a critical role in modulating swelling behavior; closer crosslink spacing restricts swelling, whereas lower solid content enhances swellability but compromises mechanical stability.[27,29]

Pore size and distribution. The polymer used (hydrophilicity) and degree of crosslinking will control the size and distribution of pores within the hydrogel matrix. In drug delivery applications, this is an important parameter controlling the rate of diffusion-controlled drug release since compounds can only diffuse when the pore size is greater than the size of the molecule.[4,30] The parameters governing drug release from the hydrogel matrix is discussed in more detail in subsequent sections.

Mechanical strength. Mechanical strength describes how well a hydrogel can maintain its structure in the swollen state. This property is particularly important in long-term drug delivery applications since the hydrogel must be able to maintain its physical structure for the intended duration of drug release. The mechanical strength can be increased by increasing the degree of crosslinking; however, altering it will also affect properties such as elasticity, swelling, and pore size.[7,27] Therefore, the correct balance between the desired strength, flexibility, water content, and pore size must be achieved.

Biocompatibility and biodegradability. Given the immune-privileged yet sensitive nature of the eye, hydrogel formulations must exhibit high biocompatibility, eliciting no cytotoxic or adverse immune responses. For this purpose, they should be formulated to be compatible with the tissue(s) they will be in contact with. For intravitreal delivery, viscosity, pH, and osmolarity should all mimic that of the vitreous.[6] Biodegradability, defined as the hydrogel's capacity to break down into non-toxic, bio-inert components under physiological conditions, is a particularly advantageous feature for intravitreal applications, as it enables safe clearance of the material without the need for surgical removal. The degradation behavior of hydrogels is influenced by several factors, including polymer molecular weight, hydrophilicity, polymer–water interactions, and environmental conditions such as pH and temperature. While many polymers undergo hydrolytic degradation in aqueous environments, some may require enzymatic or chemically catalyzed hydrolysis.[7,31] Although biodegradability is a desirable characteristic, the degradation rate must be carefully tailored to align with the intended duration of drug release and therapeutic efficacy.

Materials and methods

Search strategy

A comprehensive literature search was conducted across PubMed, Web of Science, and Scopus, following PRISMA guidelines and guided by the PICO framework. To maximize inclusivity, broad search terms were employed: (intravitreal OR intravitreous OR vitreous injection) AND (hydrogel OR in situ gel OR 3D polymer network).

Eligibility criteria

Original research articles were considered, and review articles, editorials, or conference abstracts were excluded. Only thermoresponsive gel forming systems that were intended to be intravitreally injected into the eye and carrying a therapeutic were included. Hydrogels that responded to multiple stimuli (*i.e.* light and temperature), were intended as vitreous substitutes, or were administered using microneedles were excluded due to unique variables outside of the scope of this investigation. Studies that only reported *in vivo* experiments with no *in vitro* characterization were excluded.

Data collection

All search results were imported into Covidence systematic review software (Veritas Health Innovation, Melbourne, Australia),[32] where duplicate articles were removed. Remaining papers went through two rounds of review: (1) relevance screened by title and abstract and (2) relevance screened by full text. In the first screen, papers were primarily excluded due to article type, wrong route of administration, not including a therapeutic, or not including a hydrogel. In the second screen, articles were primarily excluded for not including a thermoresponsive hydrogel, not including the necessary experimental characterizations, being a conference abstract with no full text, or including unique hydrogel components that were outside of the scope of this study (more than one triggering stimulus, hydrogel arrays, hollow cylinders, *etc.*).

Relevant characteristics of included studies were recorded, including the hydrogel materials investigated, therapeutic used, disease targeted, method of preparation, and characterizations performed. Interventions included synthetic or hybrid hydrogel systems carrying a therapeutic. The hydrogels were categorized into subgroups according to polymer origin (synthetic or hybrid). A comparative analysis of the reported physical and mechanical properties between the subgroups was conducted. Additionally, further subgroup comparisons based on therapeutic class (small molecules or proteins) and/or primary polymer components (NIPAAM, PEG, PEG-DA, PEG-PLLA-DA, PLGA-PEG-PLGA, PSHU, PCL, P407, P188, HA) were performed to assess trends based on specific components.

Risk of bias

The risk of bias for the included studies was assessed using the Cochrane Risk of Bias tool (The Cochrane Collaboration, London, United Kingdom),[33] which was custom designed to include four domains: performance bias, detection bias, confirmation bias, and measurement bias. To ensure reviewer bias didn't interfere with results, SciSpace AI (PubGenius Inc., Milpitas, CA) was used as a "second reviewer". In this case, the primary author "chatted" with each of the 35 articles and gave set prompts to obtain an objective low, medium, or high bias rating in each of the four domains. Table S1 describes each type of bias, how studies were manually classified, and the SciSpace prompts used.

For each study, if the AI-based and manual assessments differed, the paper was reexamined to review justifications and reduce bias until consensus was reached or an intermediary rating was assigned. Bias related to *in vivo* experiments was excluded, given that animal data were not evaluated in this study. Each study was assigned a score from 0–100% across four domains of bias, which were then converted into categorical rankings of low (0%), unclear (25%), moderate (50%), high (75%), or critical (100%). These values were visualized using the general robvis (risk-of-bias visualization tool).[34]

Data extraction

Data was identified and extracted manually by the primary author. All text-based extractions were confirmed using SciSpace AI, and any discrepancies were resolved through additional review of the original papers. Extracted variables included polymer components, therapeutic agent, disease target, major conclusions, swelling ratio, pore size and distribution, biocompatibility, biodegradability, reported injection volume, duration of drug release, and percentage of drug release at specified timepoints. When numerical values were not directly available in the text, they were manually extracted from published graphs using GetData Graph Digitizer (Informer Technologies Inc., Los Angeles, CA). Outcome parameters were defined as follows.

Swelling ratio, the maximum swelling capacity at 37 °C relative to the "dry" hydrogel weight. All reported swelling measurements were obtained using unloaded (drug-free) hydrogels prior to therapeutic incorporation. Pore size and distribution, assessed by microscopy to evaluate the size and consistency of pores in the hydrogel scaffold. Biocompatibility, the absence of cytotoxic effects in relevant cell lines or animal models. Biodegradability, the breakdown of the formulation into non-toxic, bioinert byproducts under physiological conditions. Injection volume, the volume of hydrogel that was injected into the vitreous or simulated vitreous models. Maximum duration of drug release, the longest duration of release reported by the authors. If studies reported multiple formulation variations or if both *in vitro* and *in vivo* results were available, the maximum release time across all reports was used. A therapeutic classification of "both" was assigned if the hydrogel was co-loaded with both a protein and small molecule drug. Percent drug release, the proportion of drug released at designated timepoints (1, 3, 5, 10, 30, 60, 90, and 120 days), with all values rounded to the nearest percent and estimated within 3% accuracy depending on figure resolution. If multiple polymer weights, injection volumes, or drug concentrations were tested within a single study, the intermediate condition was selected for inclusion in this analysis. When drug release was reported for both individual and drug combinations within the same hydrogel, the individual release values were used to maintain consistency across studies. If distinct hydrogel formulations were reported (beyond polymer, drug, or crosslinker percentage variations) then both were included. Most studies used phosphate-buffered saline (PBS) as the release medium, while a smaller

number used simulated vitreous fluid (SVF). To ensure methodological consistency across reports, PBS data were prioritized for analysis when both PBS and SVF conditions were available. Details on the specific formulations used for percent release calculations are provided in Table S2. Number of hydrogels sustaining release over time, taken as the number of hydrogels still releasing drug based on percent drug release extractions.

Data analysis

Extracted polymer characteristics without consistently reported quantitative values were summarized qualitatively. Those with quantitative data available were compared using GraphPad Prism software (Version 9.4.1; Dotmatics, Boston, MA) and represented as mean ± SD unless otherwise noted. Statistical comparisons between groups were performed using a Mann–Whitney test (two groups) or a Krusak–Wallis Test followed by Dunn's multiple comparison test (three or more groups). A significance level of $P < 0.05$ was applied.

Results

Study selection

This study adhered to the PRISMA framework, providing a structured methodology that minimizes bias and enhances reliability. A total of 504 records were initially retrieved from PubMed, Web of Science, and Scopus. After removal of 146 duplicates, 358 studies underwent title and abstract screening. Of these, 127 articles were selected for full-text review, and ultimately 35 met all inclusion criteria for quantitative synthesis. The PRISMA flow diagram (Fig. 2) provides a visual summary of the records identified, screened, excluded, and retained at each stage.

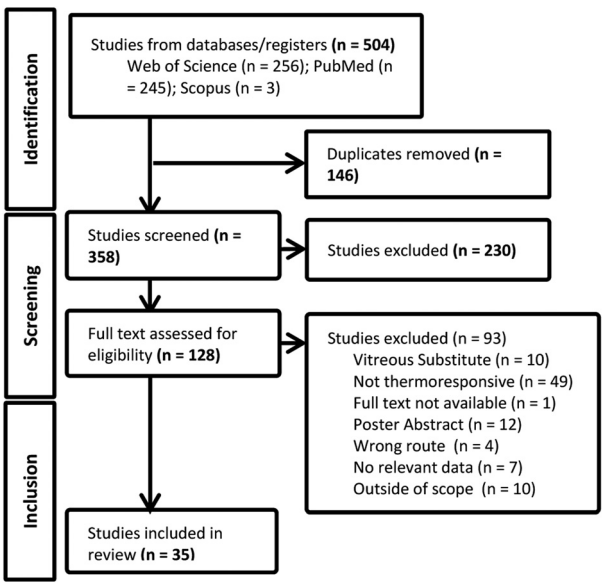

Fig. 2 PRISMA diagram for identification, screening, selection, exclusion, and retention at each stage included in this study.

Study characteristics

Tables 1, 2 and Fig. 3 summarize the hydrogel components, therapeutic agents, and principal outcomes reported across the included studies. Mechanical strength can be measured directly using specialized instrumentation; however, it is more commonly inferred from rheological behavior and/or degradation profiles. Although rheological assessments were regularly reported, differences in ambient conditions and experimental configurations greatly influence measured values.[35] Accordingly, rheological data are best suited for comparing variables within a single study, and were not used for cross-study comparisons. Subsequent sections therefore focus on parameters that are comparable between studies, including swelling ratio, pore size, biocompatibility, biodegradation, and drug-release kinetics.

Of note, tested formulations exhibited a sol-to-gel transition at physiological temperature, confirming their thermoresponsive nature and suitability for intravitreal administration. Across the dataset, key conclusions included sustained drug release, maintenance of therapeutic stability, biocompatibility *in vitro* and/or *in vivo*, and biodegradability of the hydrogel matrix. The primary disease targets addressed by these formulations were neovascularization, inflammation, and oxidative stress.

Polymer classification

Across the 35 studies included in this work, 26 investigated synthetic hydrogels and 9 evaluated hybrid systems (Fig. 3). The most common synthetic polymers were polyethylene glycol (PEG; 25.3%), *N*-isopropylacrylamide (NIPAAM; 13.8%), poloxamer 407 (P407; 9.2%), and poly(lactic-*co*-glycolic acid) (PLGA; 9.2%) (Fig. 3). Natural polymers were almost exclusively hyaluronic acid-based, owed to its native presence in the eye and its intrinsic safety and biological activity.[36] Overall, more than 20 distinct polymers were reported, underscoring the heterogeneity of existing approaches.

Therapeutic classification

For subgroup analysis, therapeutics were classified as either small molecules or proteins. Compound size is a key determinant of diffusion from the hydrogel scaffold: molecules larger than the initial mesh size can only be released once the hydrogel swells sufficiently or undergoes degradation.[9,14] While other drug properties such as charge, solubility, and functional groups also influence entrapment and release behavior, the present analysis focused on size as the primary distinguishing factor between the two subgroups. Of the 35 therapeutics included, 13 were proteins, 17 were small molecules, and 5 were hydrogels loaded with both a small molecule and protein therapeutic. Several studies incorporated additional delivery strategies, such as embedding therapeutics within micro- or nanoparticles, to further refine release kinetics (Tables 1 and 2; Fig. 3).

Table 1 Summary of preclinical studies reporting synthetic hydrogels

Study ID	Polymer components	Drug classification	Drug used[b]	Drug size[a]	Disease target	Max duration of drug release (days)	Conclusions
Ilochonwu *et al.* (2023)[37]	NIPAAM, HEA, PEG, maleimide or furan	Both	anti-VEGF antibody fragment (biosimilar to ranibizumab) or dexamethasone	48.3 kDa; 392 Da	Neovascularization and inflammation	35	■ Stable for at least one year at pH 7.4. ■ Degrades in basic pH due to hydrolysis. ■ Dexamethasone release is slower (13 days) than that of the anti-VEGF Fab fragment (35 days).
Wang *et al.* (2024)[38]	PLGA-PEG-PLGA	Both	Ciliary neurotrophic factor (CNTF); and triamcinolone acetonide	22.7–45 kDa; 435 Da	Neuroprotective and regenerative capacities to treat traumatic optic neuropathy	5	■ Preserves optic nerve. ■ High delivery efficacy and sustained drug release. ■ Mechanical properties consistent with that of the vitreum.
Rudeen *et al.* (2022)[39]	NIPAAM, PEG-PLLA-DA	Both	Aflibercept Microparticles[a] and dexamethasone nanoparticles[a]	115 kDa; 392 Da	Neovascularization	224	■ Hydrogel extends and controls dual drug release. ■ Bioactivity maintained.
Awwad *et al.* (2018)[40]	NIPAAM, PEG-DA	Protein	Bevacizumab or PEG conjugated ranibizumab	149 kDa; 48.3 kDa	Neovascularization	17	■ *In situ* loaded hydrogels provide prolonged release profiles. ■ Modified protein (PEG10-Fabrani) has better incorporation within the hydrogel matrix than unmodified protein owed to PEG entanglement and compatibility.
Rauck *et al.* (2014)[41]	ESHU (PEG-PSHU)	Protein	Bevacizumab	149 kDa	Neovascularization	63	■ Sustained bevacizumab release for over 9 weeks. ■ Achieved ocular concentrations 4.7 times greater than bolus injections. ■ The gel did not affect intraocular pressure.
Hu *et al.* (2014)[42]	mPEG-PLGA-BOX	Protein	Bevacizumab	149 kDa	Neovascularization	30	■ Bioactivity maintained during the release process.
Liu *et al.* (2019)[43]	NIPAAM, PEG-PLLA-DA	Protein	Aflibercept loaded PLGA microspheres[a]	115 kDa	Neovascularization	204	■ Controlled aflibercept release while maintaining bioactivity for 6 months. ■ Amount and rate of drug release can be controlled by the loaded cross-linker and drug amount.
Osswald *et al.* (2016)[44]	NIPAAM, PEG-DA	Protein	Ranibizumab or aflibercept loaded PLGA microparticles[a]	48.3 kDa; 115 kDa	Neovascularization	196	■ Bioactivity of drugs is maintained throughout the release period. ■ Hydrogel significantly reduces initial burst and extends drug release.
Xie *et al.* (2015)[45]	PLGA-PEG-PLGA	Protein	Bevacizumab	149 kDa	Neovascularization	14	■ Increased drug loading lowers sol-gel transition temperature. ■ Extended drug release into the vitreous humor and retina.
Wang *et al.* (2012)[46]	PEOz-PCL-PEOz	Protein	Bevacizumab	149 kDa	Neovascularization	20	■ Reversible sol–gel transition ■ Extended drug release.

Table 1 *(Contd.)*

Study ID	Polymer components	Drug classification	Drug used[b]	Drug size[a]	Disease target	Max duration of drug release (days)	Conclusions
Kang Derwent *et al.* (2008)[47]	NIPAAM, PEG-DA	Protein	Bovine serum albumin, IgG, bevacizumab or ranibizumab	66.4 kDa; 150 kDa; 149 kDa; 48.3 kDa	Neovascularization	21	■ Fast, reversible phase changes with temperature. ■ Protein release can be adjusted by cross-link density. ■ High protein encapsulation. ■ Initial burst release occurs within 48 hours.
Xue *et al.* (2019)[48]	PEG, PPG, PCL	Protein	Bevacizumab, aflibercept, or FITC-rabbit IgG	149 kDa; 115 kDa; 150 kDa	Neovascularization	40	■ Varying the hydrophilic/lipophilic balance can alter the drug release rate. ■ The released anti-VEGFs remain active for up to 40 days.
Patel *et al.* (2014)[49]	PCL, PEG, PLLA	Protein	IgG	150 kDa	Neovascularization	25	■ Easy to handle at room temperature. ■ Sustained release of IgG.
du Toit *et al.* (2021)[50]	PEG-PCL-PEG/P407	Small molecule	p11 anti-angiogenic peptide in PLGA nanoparticles[a]	721 Da	Neovascularization	60	■ 67% peptide loading efficiency.
Prosperi-Porta *et al.* (2017)[51]	NIPAAM, NAS, DBA, AAm	Small molecule	Dexamethasone	392 Da	Inflammation	100	■ Increased AAm/DBA ratio enhances drug release rates. ■ Higher molecular weight increases drug encapsulation efficiency. ■ Copolymer degradation occurs *via* hydrolytic ring opening of DBA.
Aragón-Navas *et al.* (2024)[52]	PLGA-PEG-PLGA	Small molecule	Dexamethasone-phosphate	472 Da	Inflammation	21	■ PLGA-PEG-PLGA hydrogels suitable for long-term intravitreal treatments. ■ Preliminary studies showed faster wound healing with hydrogels.
Pachis *et al.* (2017)[53]	P407	Small molecule	Flurbiprofen liposomes[a]	244 Da	Inflammation	4	■ Increased ocular bioavailability and extended retention time in the vitreous.
Annala *et al.* (2023)[54]	NIPAAM, NAS, PEG	Small molecule	Dexamethasone with methacrylated thioether	392 Da	Inflammation	430	■ Dexamethasone was released in its native form with limited degradation products formed. ■ The hydrogel maintained therapeutic levels for over 500 days.
Sapino *et al.* (2019)[55]	P407	Small molecule	Cefuroxime solid lipid nanoparticles or microemulsion[a]	424 Da	Inflammation	7	■ Drug stable for over 1 month.
López-Cano *et al.* (2021)[56]	PLGA-PEG-PLGA	Small molecule	Dexamethasone and ketorolac alone or in combination with antioxidants idebenone and D-α-tocopherol polyethylene glycol 1000 succinate (TPGS)	392 Da; 255 Da; 338 Da; 530 Da	Inflammation and oxidative stress	62	■ Sustained drug release over 47 to 62 days. ■ Well tolerated in retinal cells. ■ High oxidative protection and reduced TNF-α production.
Zou *et al.* (2019)[57]	NIPAAM, MAA, HEMA, PTMC	Small molecule	Indomethacin	358 Da	Inflammation	14	■ Drug release was controlled by hydrogel degradation and diffusion.
Wang *et al.* (2023)[58]	PLGA-PEG-PLGA	Small molecule	3BDO and trichostatin (TSA)	327 Da; 302 Da	Targets mTOR and HDAC to treat traumatic optic neuropathy	28	■ Effectively induces optic nerve repair and improved visual function. ■ Drug delivery system overcomes multiple inhibitory signals. ■ Sustained delivery and enhanced treatment efficacy.

Table 1 *(Contd.)*

Study ID	Polymer components	Drug classification	Drug used[b]	Drug size[a]	Disease target	Max duration of drug release (days)	Conclusions
Huang *et al.* (2023)[59]	PLGA-PEG-PLGA	Small molecule	Dexamethasone and berberine (BBR)-loaded mesoporous silica nanoparticles (MSNs)[a]	392 Da; 336 Da	Inflammation	42	■ Sustained drug release over 6 weeks and enhanced treatment efficacy. ■ Anti-inflammatory *in vitro* and *in vivo*.
Zhang *et al.* (2015)[60]	PLGA-PEG-PLGA	Small molecule	Dexamethasone	392 Da	Inflammation	18	■ Drug diffusion and gel erosion control dexamethasone release. ■ Sustained release and lengthened ocular retention.
Famili *et al.* (2014)[61]	NIPAAM, PSHU	Small molecule	Triamcinolone acetonide	394 Da	Inflammation	60	■ Biodegradability mechanisms can apply to various NIPAAM systems. ■ Combined system offers sustained release for up to a year.
Wang *et al.* (2018)[62]	PBLA-PEG-PBLA	Small molecule	Ganciclovir	255 Da	Antiviral to treat cytomegalovirus (CMV) retinitis	6	■ Favorable physicochemical properties for ocular application. ■ Enhanced pharmacokinetics were observed in CMV retinitis treatment. ■ Prolonged drug release and enhanced ocular bioavailability. ■ Good stability.

[a] All drug sizes were obtained from Drug Bank Database,[63] study methods, or manufacturer data sheets. [b] Indicates use of micro- or nanosized drug formulations

Hydrogel properties

Swelling ratio. The degree of swelling reflects a hydrogel's capacity to absorb and retain water following injection. As swelling increases, expansion of the internal pore network occurs, directly influencing the diffusion of entrapped therapeutics through the polymer matrix. Swelling behavior is therefore a critical determinant of drug-release performance and must be carefully evaluated during hydrogel design.[28]

Methodologies used to determine swelling ratios varied substantially across studies (Table 3). Some studies measured hydrogel "dry" weight immediately after preparation, whereas others employed lyophilization prior to weighing. Additionally, two distinct equations were used to calculate swelling ratios. To ensure comparability, only studies using consistent drying methods and calculation equations were pooled for analysis. Studies that weighed hydrogels immediately after preparation and calculated swelling ratio as W_{wet}/W_{dry} are shown in Fig. 4A (method 1), while those that lyophilized hydrogels and calculated swelling ratio as $(W_{wet} - W_{dry})/W_{dry}$ are shown in Fig. 4B (method 2).

No significant differences were observed between synthetic and hybrid formulations, suggesting that polymer class alone does not strongly influence swelling behavior (Fig. 4). Because swelling is primarily governed by crosslink density and network structure, parameters such as polymer concentration and preparation method likely exert greater influence than polymer origin.[7,27] Notably, mean swelling ratios differed between methodologies, with values of 2.29 ± 0.88 for method 1 and 3.77 ± 1.76 for method 2. Given these methodological differences and resulting variability, caution is warranted when comparing swelling data across studies.

Pore size and distribution. The size and density of pores within the hydrogel scaffold is critical for diffusion-controlled release, as compounds can only diffuse once the pore size exceeds the molecular dimensions of the therapeutic.[4,30] Among the studies included in this analysis, fewer than half reported microscopy data, and only seven investigations provided quantitative measurements. Reported morphologies varied widely depending on polymer type, therapeutic cargo, and preparation method. Most studies described hydrogels with well-defined porous structures, ranging from the nanometer to micrometer scale (synthetic: 0.1–150 μm; hybrid: 0.02–10 μm), which supported sustained drug release and structural stability (Table 4). Pore size and distribution were consistently linked to drug release kinetics: larger, interconnected pores facilitated faster diffusion, whereas denser, more homogeneous networks prolonged release.

The reliability of these analyses remains limited by potential artifacts introduced during sample preparation. Scanning electron microscopy (SEM) was the most frequently reported technique among the included studies; however, caution is warranted when interpreting results, as the rapid freeze-drying process required for SEM visualization can distort or collapse the native pore structure. In contrast, cryo-SEM and transmission electron microscopy (TEM) offer superior preservation

Table 2 Summary of preclinical studies reporting hybrid hydrogels

Study ID	Polymer components	Drug classification	Drug used[b]	Drug size[a]	Disease target	Max duration of drug release (days)	Conclusions
Jiang *et al.* (2025)[64]	P407, HA	Both	Rapamycin-loaded microemulsion[a] and ranibizumab	914 Da; 48.3 kDa	Neovascularization and mTOR/oxidative stress	7	■ Enhanced drug efficacy. ■ Synergistic drug delivery system disrupts pathways that promote angiogenesis. ■ Improved therapeutic outcomes with a more precise control of treatment window. ■ Deep penetration into posterior eye segment with accumulation in RPE for at least 14 days.
Taheri *et al.* (2022)[65]	P407, HPMC K15M	Both	Dexamethasone and/or bevacizumab-loaded CNAC (chitosan-*N*-acetyl-L-cysteine) nanoparticles[a]	392 Da; 149 kDa	Neovascularization and inflammation	10.67	■ Improved therapeutic efficacy with fewer required doses. ■ Prevented initial burst and prolonged drug release.
Awwad *et al.* (2019)[66]	NIPAAM, acrylated HA	Protein	Infliximab or bevacizumab	144.2 kDa; 149 kDa	Neovascularization	50	■ Biodegradable, degradation is influenced by hyaluronidase concentration. ■ Antibody remained stable during hydrogel polymerization. ■ Bioactivity maintained throughout study period suggesting protein stability. ■ Therapeutic dose maintained in posterior segment of the eye.
Egbu *et al.* (2018)[67]	PEG-DA-NIPAAM-HA	Protein	Infliximab	144.2 kDa	Inhibits tumor necrosis factor-alpha (TNF-α) targeting AMD	12	■ Potential for prolonged intraocular protein release. ■ Sustained release profiles compared to free protein.
Bakhrushina *et al.* (2023)[68]	P407, P188, HA, PEG, ascorbic acid	Small molecule	Cefuroxime	424 Da	Endophthalmitis	3	■ Prolonged drug release and stability.
Xiong *et al.* (2018)[69]	D-Glu, SA	Small molecule	Triamcinolone acetonide (TA)	394 Da	Inflammation	3	■ Effectively controlled noninfectious uveitis.
Liu *et al.* (2024)[70]	P407, HA, P188	Small molecule	Borneol-decorated paeoniflorin & tetramethylpyrazine-coloaded microemulsions[a]	480 Da; 136 Da	Neovascularization and oxidative stress	21	■ Significant reduction in choroidal neovascularization and enhanced therapeutic efficacy.
Su *et al.* (2023)[71]	P407, P188, HA	Small molecule	Borneol-decorated rhein and baicalein-coloaded microemulsions[a]	284 Da; 270 Da	Neovascularization and oxidative stress	14	■ Deep penetration in the posterior ocular segment is achieved. ■ Superior inhibition of CNV in wAMD mouse model is demonstrated.
Delplace *et al.* (2019)[72]	HA, MC	Protein	Ciliary neurotrophic factor (CNTF) + maleimide-modified SH3-binding peptide	22.7–45 kDa	Retinal neuroprotection	7	■ Sustained protein release to the retina while maintaining bioactivity. ■ The delivery system demonstrates safety for intravitreal applications.

[a] All drug sizes were obtained from Drug Bank Database,[63] study methods, or manufacturer data sheets. [b] Indicates use of micro- or nanosized drug formulations.

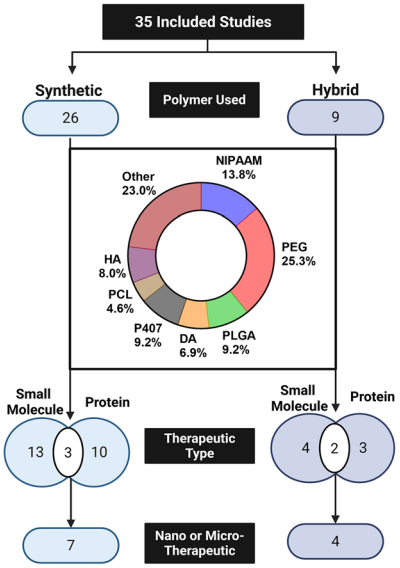

Fig. 3 Summary of included studies based on the polymer and therapeutic used to form thermoresponsive hydrogels Created in BioRender. Beathard, A. (2026). https://BioRender.com/qhen7bh. DA: diacrylate; NIPAAM: *N*-isopropylacrylamide; P188: poloxamer 188 (pluronic F-68); P407: poloxamer 407 (pluronic F-127); PCL: poly(ε-caprolactone); PEG: poly(ethylene glycol); PLGA: poly(lactic-*co*-glycolic acid); HA: hyaluronan/hyaluronic acid.

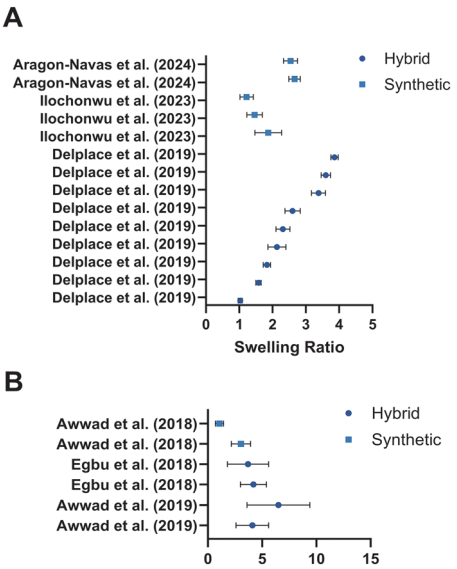

Fig. 4 Swelling ratios of synthetic and hybrid hydrogels determined using (A) experimental method 1 and (B) experimental method 2.

of the gel's native morphology, though both demand more complex preparation procedures and specialized instrumentation.[73] Wider adoption of advanced imaging modalities would enhance formulation optimization by enabling precise correlation between pore size, network density, and therapeutic size, therefore facilitating rational tuning of hydrogel structures to achieve desired drug-release durations.

Biocompatibility and biodegradation. For clinical translation, it is essential that hydrogels exhibit biocompatibility, eliciting no cytotoxic or inflammatory responses, and undergo biodegradation into non-toxic byproducts enabling safe clearance from ocular tissues following drug release.[6] Of the 35 studies included, 30 evaluated safety using *in vitro* assays (*e.g.*, MTT, alamar blue, LDH, live/dead cell screens) in cell lines such as ARPE-19, HUVEC, RAW 264.7, and RPE-1, and/or through *in vivo* studies (Fig. 5). Across the multitude of different polymers and therapeutics assessed, reports consistently demonstrated negligible toxicity, strong cytocompatibility, and absence of inflammatory responses (Tables 5 and 6). Because degradation is influenced by multiple factors, including polymer molecular weight and component ratios, it must be experimentally verified for each new formulation. Beyond safety, degradation impacts the rate and extent of drug release, making it an important component in obtaining desired release profiles.[7,31] Despite this, only 13 of the 35 studies reported degradation data, and most ended evaluations before complete breakdown. Synthetic formulations typically exhibited slower, more controlled degradation, ranging from several weeks[52,57,62] to many months[41,43] (Table 5). In contrast, the two hybrid formulations that reported degradation data showed substantial breakdown (19–73%) within 1–4 days[65,66] (Table 6).

Table 3 Experimental details for swelling ratio calculation

Study ID	Temperature	Initial weight determination	Equation used to calculate swelling ratio[a]	Included in analysis?
Ilochonwu *et al.* (2023)[37]	37 °C	Immediately after preparation	$Q = W_{wet}/W_{dry}$	Yes: Method 1
Delplace *et al.* (2019)[72]	37 °C	Immediately after preparation	$Q = W_{wet}/W_{dry}$	Yes: Method 1
Aragón-Navas *et al.* (2024)[52]	37 °C	Immediately after preparation	$Q = W_{wet}/W_{dry}$	Yes: Method 1
Awwad *et al.* (2019)[66]	25 and 37 °C	Lyophilized	$Q = (W_{wet} - W_{dry})/W_{dry}$	Yes: Method 2
Awwad *et al.* (2018)[40]	25, 37, and 48 °C	Lyophilized	$Q = (W_{wet} - W_{dry})/W_{dry}$	Yes: Method 2
Egbu *et al.* (2018)[67]	25 and 37 °C	Lyophilized	$Q = (W_{wet} - W_{dry})/W_{dry}$	Yes: Method 2
du Toit *et al.* (2021)[50]	37 °C	Immediately after preparation	$Q = (H_{wet} - H_{dry})/H_{dry}$	No
Kang Derwent *et al.* (2008)[47]	25 and 37 °C	Unclear	Not reported	No
Rudeen *et al.* (2022)[39]	22 °C to 46 °C	Lyophilized	$Q = W_{wetwet}/W_{dry}$	No
Annala *et al.* (2023)[54]	37 °C	Immediately after preparation	Not reported	No

[a] W_{wet} = hydrogel weight in swollen state; W_{dry} = initial hydrogel weight; H_{wet} = hydrogel height in swollen state; H_{dry} = initial hydrogel height.

Table 4 Pore size and distribution of hydrogel formulations

Study ID	Therapeutic type	Polymer type	Pore size/distribution
Ilochonwu *et al.* (2023)[37]	Both	Synthetic	SEM: Empty hydrogels exhibited small, interconnected pores; protein-loaded hydrogels had larger pores with smaller interconnected pores; Dex-loaded hydrogels displayed heterogeneous structures.
Liu *et al.* (2019)[43]	Protein	Synthetic	SEM: ~100 nm at room temperature, homogeneous; collapsed at body temperature with a denser distribution and rougher surfaces observed.
Xie *et al.* (2015)[45]	Protein	Synthetic	SEM: 3D porous structure (100–150 μm) in PLGA-PEG-PLGA hydrogels enabled diffusion-based release of Avastin.
Wang *et al.* (2012)[46]	Protein	Synthetic	SEM: Cross-sections showed exposed fibers; erosion over 50 days increased pore size from 10–20 μm to larger, more numerous pores.
Kang Derwent *et al.* (2008)[47]	Protein	Synthetic	Bright-field microscopy: Uniform pore surface formed by cross-linking.
Xue *et al.* (2019)[48]	Protein	Synthetic	Confocal: Protein domain size decreased with more hydrophilic PEG : PPG ratios; smaller, more homogeneous pores correlated with slower protein release.
Zou *et al.* (2019)[57]	Small molecule	Synthetic	SEM: Pores 2–10 μm; porosity and size dependent on hydrogel formulation; smaller pores correlated with slower indomethacin release.
Wang *et al.* (2018)[62]	Small molecule	Synthetic	Light microscopy: Higher copolymer concentration produced fewer, irregular pores, slowing drug release compared to lower concentration gels.
Su *et al.* (2023)[71]	Small molecule	Hybrid	SEM: Temperature-responsive hydrogel (TRG) showed 3D porous structure; Bor/RB-M loading caused roughened inner pore walls.
Xiong *et al.* (2018)[69]	Small molecule	Hybrid	TEM: TA-SA-Glu hydrogels formed nanofibrous structures (~20 nm diameter, several microns long) entangled to create stable supramolecular hydrogels.
Egbu *et al.* (2018)[67]	Protein	Hybrid	SEM: PEGDA-pNIPAAM-HA gels had well defined pores (1–2 μm).
Liu *et al.* (2024)[70]	Small molecule	Hybrid	SEM: Bor/PT-M@TRG hydrogels showed porous network with ~10 μm pores.

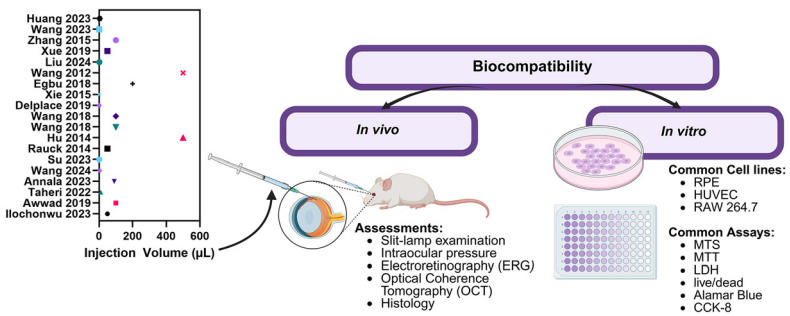

Fig. 5 Summary of hydrogel volumes injected, and biocompatibility assessments performed. Created in BioRender. Beathard, A. (2026). https://BioRender.com/4wn3u6p.

Injection volume. From a clinical standpoint, the volume of an intravitreal injection plays a critical role in patient safety and therapeutic efficacy. Larger injected volumes are associated with greater transient increases in intraocular pressure, but injecting too small a volume may limit drug exposure, reduce distribution, or compromise efficacy.[74] Thus, volumes must be large enough to deliver a therapeutic dose, yet small enough to avoid undue risk. The mean injection volume reported across included studies was 98.18 ± 151.40 μL (n = 19), with a median of 50 μL (Fig. 5). This aligns with current clinical practice, where the standard intravitreal injection volume is 50 μL, and the largest recommended range is 100–200 μL.[75] However, there was substantial heterogeneity across studies with volumes ranging between 1 and 500 μL. Conclusions drawn regarding biocompatibility based on *in vivo* work (Tables 5 and 6) could be insufficient if injection volumes are substantially lower than what is required for clinical use. Moreover, inconsistent injection volumes make comparisons between studies difficult, as changes in intraocular pressure, retinal thickness, other measures of safety, and efficacy determinations will be impacted.

Risk of bias assessment. Of the 35 included studies, only one demonstrated a high risk of bias in a single domain (Fig. 6). The most common source of bias was detection bias, with four studies (11.4%) rated as unclear due to insufficient methodological detail. To determine whether these studies disproportionately influenced the overall findings, a sensitivity analysis was performed in which studies with an unclear or high risk of bias in any domain were excluded. The average maximum duration of drug release for synthetic and hybrid systems was then compared with and without these studies. As shown in Fig. S1, exclusion of these studies did not significantly alter the reported release durations. This finding suggests that although some methodological details were insufficiently reported, their inclusion did not meaningfully bias the overall analysis. Therefore, these studies were retained

Table 5 Biodegradability and biocompatibility of synthetic hydrogels

Study ID	Polymer components	Biodegradability	Biocompatibility/toxicity test and cell line	Compatibility conclusion
Ilochonwu *et al.* (2023)[37]	NIPAAM, HEA, PEG, maleimide or furan	Gels degrade at basic pH levels of 10 and 11, with degradation occurring after 13 days and 3 days, respectively. Hydrogel degradation is slow at a neutral pH.	Alamar blue assay and live/dead cell screen; ARPE-19 cells and RAW 264.7 macrophages.	Cytocompatible with no observed toxic effects.
Wang *et al.* (2024)[38]	PLGA-PEG-PLGA	Not reported.	CCK-8 assay and live/dead cell screen; primary RGC, RPE, and muller cells.	Good cytocompatibility with viability comparable to positive control group.
Rudeen *et al.* (2022)[39]	NIPAAM, PEG-PLLA-DA	Not reported.	Not reported.	Not reported.
Awwad *et al.* (2018)[40]	PEG-DA, NIPAAM	Not reported.	Not reported.	Not reported.
Rauck *et al.* (2014)[41]	ESHU (PEG-PSHU)	10% and 20% degradation after 45 days, in the absence and presence of cholesterol esterase, respectively.	Live/dead cell screen; bovine corneal endothelial cells. *In vivo* studies.	Confirmed biocompatibility *in vitro* and *in vivo*.
Hu *et al.* (2014)[42]	mPEG-PLGA-BOX	Not reported.	MTT assay; HUVEC and Macaca mulatta retina epithelial cells. *In vivo* studies.	Nontoxic to ocular tissue *in vivo*.
Liu *et al.* (2019)[43]	NIPAAM, PEG-PLLA-DA	54–62% degradation at 220 days depending on the polymer concentration.	Live/dead cell screen; HUVEC.	Safe and biocompatible with human cells.
Osswald *et al.* (2016)[44]	NIPAAM, PEG-DA	Not reported.	MTS assay; HUVEC.	No toxicity.
Xie *et al.* (2015)[45]	PLGA-PEG-PLGA	Volume of the hydrogel in the vitreous humor gradually decreased *in vivo*, with almost complete disappearance at 8 weeks. No apparent toxicity suggesting safe byproducts.	*In vivo* studies.	Biocompatible with retinal tissue with no long-term effects on function.
Wang *et al.* (2012)[46]	PEOz-PCL-PEOz	Increase in pore size by 50 days suggesting erosion of polymer matrix. No toxicity observed within 2 months.	Propidium iodide assay; ARPE-19. *In vivo* studies.	Good *in vitro* and intraocular biocompatibility.
du Toit *et al.* (2021)[50]	PEG-PCL-PEG/P407	Not reported.	MTT assay; RPE-1 cells.	Biocompatible.
Kang Derwent *et al.* (2008)[47]	NIPAAM, PEG-DA	Not reported.	MTS assay; HUVEC.	No toxicity after hydrogel is thoroughly washed.
Xue *et al.* (2019)[48]	PEG, PPG, PCL	Not reported.	LDH assay; HUVEC.	No toxicity.
Patel *et al.* (2014)[49]	PCL, PEG, PLLA	Not reported.	Cytokine ELISAs, MTS, and LDH assay; ARPE-19 cells.	Negligible toxicity and excellent safety. Absence of inflammatory mediators.
Prosperi-Porta *et al.* (2017)[51]	NIPAAM, NAS, DBA, AAm	Not reported.	MTT assay and live/dead cell screen; RPE-19 cells.	Good biocompatibility.
Aragón-Navas *et al.* (2024)[52]	PLGA-PEG-PLGA	PPP1500 formulations were approximately 30% degraded by day 14. All polymer byproducts are stated to be safe.	Trypan blue viability assay; RPE-1 cells.	Good viability observed with no differences between treatment and control.
Pachis *et al.* (2017)[53]	P407	3–12% degradation by 50 days.	*In vivo* studies.	No observed toxicity.
Annala *et al.* (2023)[54]	NIPAAM, NAS, PEG	Triggered cleavage of polymer bonds after addition of TCEP. It is expected that natural redox system in the eye will slowly degrade polymer, but vitreous conditions are not tested in the study.	Alamar blue assay and live/dead cell screen; ARPE-19 cells.	Good cytocompatibility.
Sapino *et al.* (2019)[55]	P407	Not reported.	SRB assay; ARPE-19 cells.	Biocompatible.
López-Cano (2021)[56]	PLGA-PEG-PLGA	Not reported.	MTT assay; RPE-1 cells.	HyG-1 formulation is well tolerated.
Zou *et al.* (2019)[57]	NIPAAM, MAA, HEMA, PTMC	60–62% degraded by day 18.	CCK-8 assay; mouse fibroblasts (L929). *In vivo* studies.	Good *in vitro* and *in vivo* biocompatibility.
Wang *et al.* (2023)[58]	PLGA-PEG-PLGA	Not reported.	*In vivo* studies.	No noticeable effects to the retina, highlighting safety.
Huang *et al.* (2023)[59]	PLGA-PEG-PLGA	Not reported.	CCK-8 and live/dead cell screen; human conjunctival epithelial cells. *In vivo* studies.	High biological safety with negligible cytotoxicity observed.
Zhang *et al.* (2015)[60]	PLGA-PEG-PLGA	Not reported.	*In vivo* studies.	Good biocompatibility with no toxicity observed.
Famili *et al.* (2014)[61]	NIPAAM, PSHU	Polymer degradation and clearance with significant mass loss at day 1 and 3 using an accelerated degradation study.	MTT assay; ARPE-19 cells. *In vivo* studies.	No decrease in cell metabolic activity and no toxicity observed *in vivo*.
Wang *et al.* (2018)[62]	PBLA-PEG-PBLA	After day 2, 2% degradation occurred per day. Over 50% of the amount of hydrogel was degraded by day 14.	*In vivo* studies.	Acceptable biocompatibility with no inflammatory responses observed.

Table 6 Biodegradability and biocompatibility of hybrid hydrogels

Study ID	Polymer components	Biodegradability	Biocompatibility/toxicity test and cell line	Biocompatibility/toxicity conclusion
Jiang *et al.* (2025)[64]	P407, HA	Not reported.	MTT assay; ARPE-19 cells.	Minimal cytotoxicity observed.
Taheri *et al.* (2022)[65]	P407, HPMC K15M	36% (drug loaded) or 65% (empty hydrogel) degraded within 24 hours.	MTT assay; HUVEC.	Confirmed biocompatibility *in vitro* and *in vivo*.
Awwad *et al.* (2019)[66]	NIPAAM, acrylated HA	19–73% degraded by day 4.	Not reported.	Not reported.
Egbu *et al.* (2018)[67]	PEG-DA-NIPAAM-HA	Not reported.	Not reported.	Not reported.
Bakhrushina *et al.* (2023)[68]	P407, P188, HA, PEG, Ascorbic acid	Not reported.	HET-CAM test.	Absence of irritating effects on the mucosa
Xiong *et al.* (2018)[69]	D-Glu, SA	Not reported.	MTT assay; ARPE-19 cells and RAW264.7 macrophages.	Excellent intraocular biocompatibility with no observed retinal toxicity.
Liu *et al.* (2024)[70]	P407, HA, P188	Not reported.	CCK-8 assay; HUVEC and ARPE-19 cells. *In vivo* studies.	No observed retinal damage.
Su *et al.* (2023)[71]	P407, P188, HA	Not reported.	MTT assay; ARPE-19 cells. *In vivo* studies.	Acceptable biocompatibility.
Delplace *et al.* (2019)[72]	HA, MC	Not reported.	*In vivo* studies.	The retinal structure was preserved and the outer nuclear layer (ONL) thickness maintained after treatment.

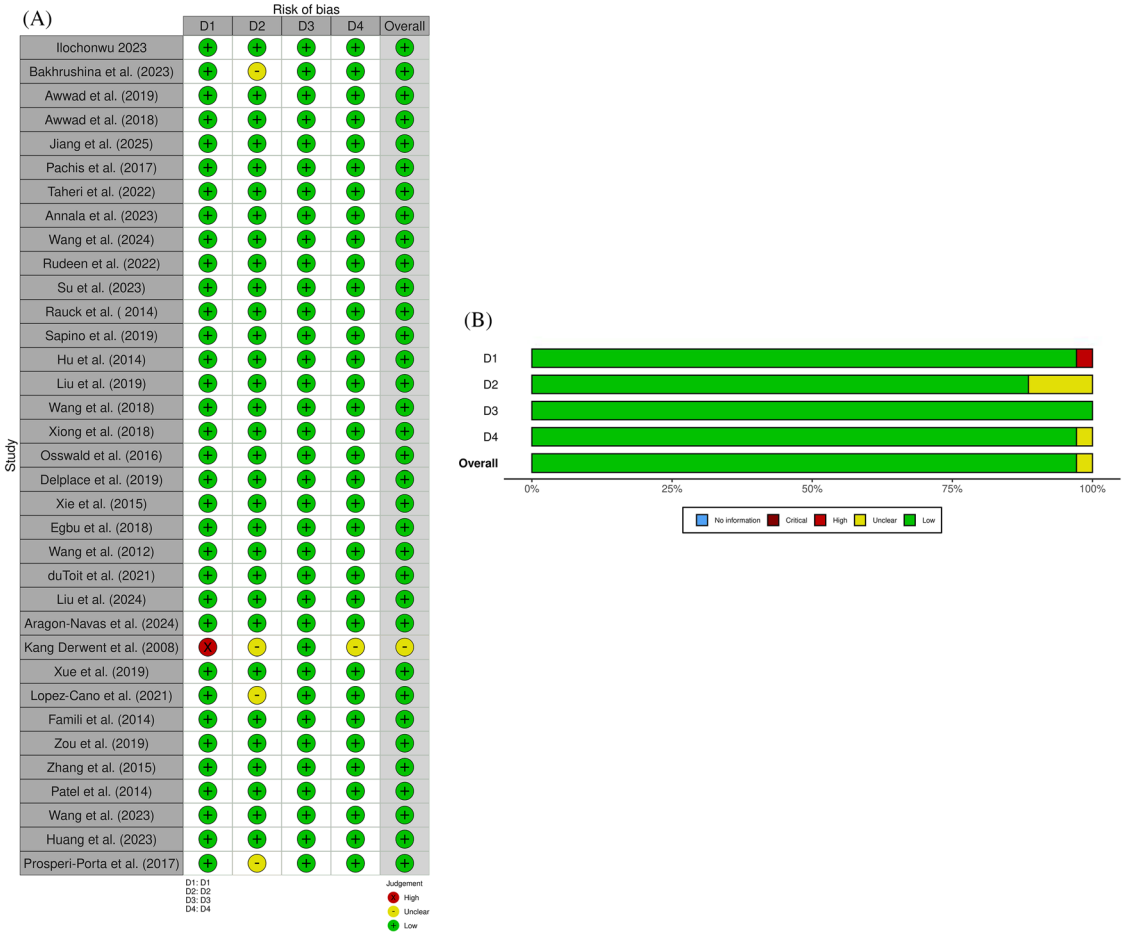

Fig. 6 Risk of bias assessment for the included studies: (A) detailed study-level evaluation and (B) overall summary across all studies. Bias domains include (D1) performance bias, (D2) detection bias, (D3) measurement bias, and (D4) confirmation bias. Visualizations were generated using the robvis (risk-of-bias visualization) tool.

in the final dataset. Overall, the low incidence of bias, use of dual-reviewer assessment, and confirmation through sensitivity analysis support the robustness of the synthesized results.

Maximum duration of drug release. Drug release durations across the included studies ranged from several days to over one year, with all hydrogel formulations extending release compared to drug alone. On average, synthetic hydrogels provided significantly longer maximum release durations compared to hybrids (62.0 ± 91.0 days and 14.2 ± 14.6 days, respectively; P = 0.01) (Fig. 7A). While average release durations did not differ significantly between micronized and non-micronized formulations (Fig. 7B), direct comparisons have previously demonstrated that combining size reduction with hydrogel delivery can significantly prolong drug release.[65] Of the four synthetic hydrogel systems capable of sustaining release beyond six months, three incorporated nano- or microsized therapeutics, underscoring the added benefit of integrating size reduction strategies within hydrogel scaffolds (Table 1).

When comparing therapeutic class within synthetic systems, no notable differences were observed between proteins and small molecules (53.8 and 58.5 days respectively; Fig. 7C). In contrast, hybrid systems demonstrated longer mean release times for proteins (23.0 days) compared to small molecules (10.3 days) (Fig. 7E). For synthetic hydrogels, the longest mean release times were observed with NIPAAM (130.1 days), PEG (94.1 days), PEG-DA (78.0 days), PEG-PLLA-DA (214.0 days), and NAS (265.0 days) (Fig. 7D). Notably, the only hybrid formulation capable of sustaining drug release beyond 21 days required chemical modifications to HA, underscoring that substantial chemical and formulation strategies are necessary to improve durability when natural polymers are used (Fig. 7F).[66]

Cumulative percent drug release. The cumulative percent of drug released at different timepoints (1, 3, 5, 10, 30, 60, 90, and 120 days) was assessed for all studies reporting *in vitro* drug release (Fig. 8). Synthetic hydrogels demonstrated a gradual and sustained release profile over time. On day 1, the mean release was 22.3% ± 19.8 (n = 34), increasing steadily to 39.9% ± 23.3 (n = 33) by day 5 and 47.8% ± 24.9 (n = 30) by day 10. Later timepoints showed stabilization, with release plateauing near 58.9% ± 28.7 (n = 22) at 30 days and 56.7% ± 31.7 (n = 12) at 60 days. The 5 hydrogels that continued to release drug at later timepoints (38.6% at day 90; 43.6% at day 120), demonstrated slower, controlled release over several months. Hybrid hydrogels exhibited more variability. On day 1, release averaged 49.6% ± 31.5 (n = 17) and continued to increase through day 3 (57.1% ± 30.6, n = 15). However, only 6 of the 17 original formulations sustained release past the 3-day timepoint. The release was slower for the remaining hydrogels, with 48.7% ± 31.4 (n = 6) at day 5 and 24.5% ± 0.71 (n = 2) at day 10 (Fig. 8B). When comparing therapeutic subclasses, synthetic hydrogels performed similarly for both small molecule and protein drugs. Small molecules demonstrated release of 20.5% ± 19.4 (n = 20) at day 1, rising to 39.3% ± 24.3 (n = 20) by day 5 and 50.8% ± 28.6 (n = 12) by day 30. Protein-loaded synthetics showed comparable trends: 24.9% ± 20.9 (n = 14) at day 1,

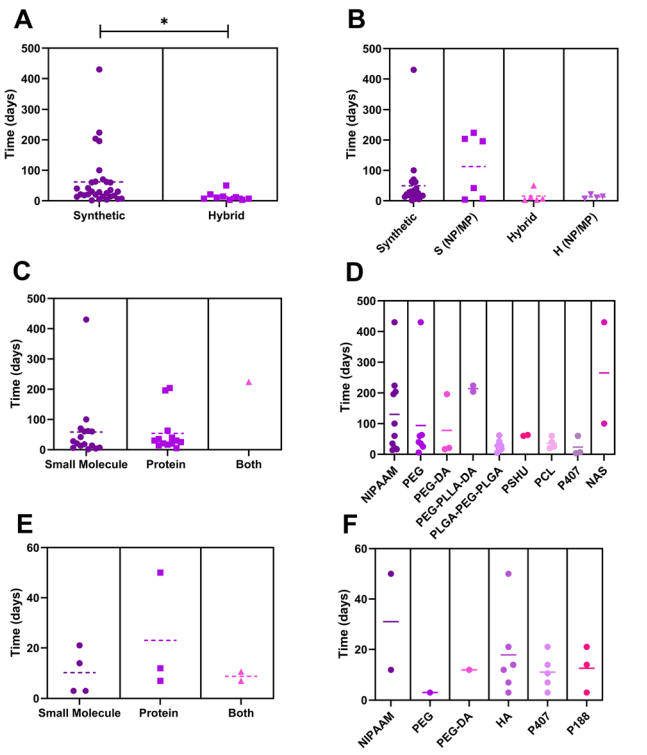

Fig. 7 Maximum reported duration of drug release for: (A) polymer class; (B) polymer class and use of nano/microparticles; (C) therapeutic, synthetic hydrogels; (D) polymers, synthetic hydrogels; (E) therapeutic, hybrid hydrogels; and (F) polymers, hybrid hydrogels.

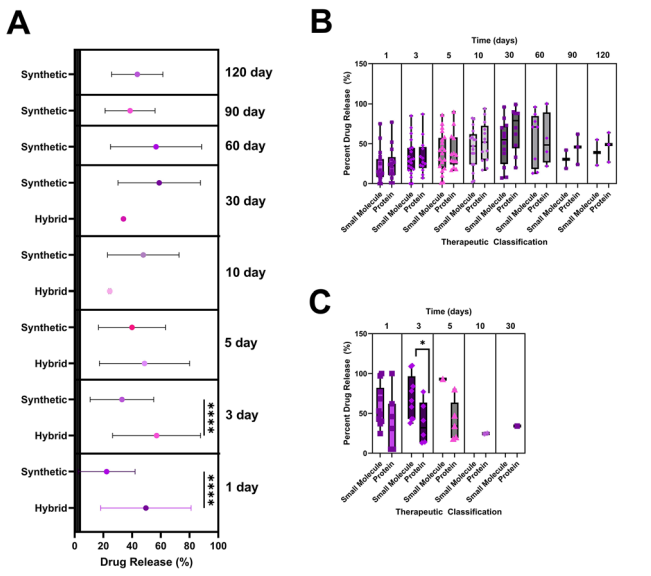

Fig. 8 Cumulative percent release for: (A) all hydrogels; (B) synthetic hydrogels; and (C) hybrid hydrogels. Box plots for each timepoint are separated by small molecules (left) and proteins (right). *P < 0.05; ****P < 0.0001.

40.9% ± 22.8 (n = 13) by day 5, and 68.6% ± 27.1 (n = 10) at day 30 (Fig. 8C). Both subclasses retained meaningful release through day 120, suggesting synthetic matrices can accommodate different therapeutic sizes without major differences in performance. In contrast, small molecule-loaded hybrids released drugs rapidly, reaching 58.9% ± 25.7 (n = 10) by day 1 and increasing to 93.0% (n = 1) by day 5. Protein-loaded hybrids demonstrated more controlled release, starting at 36.3% ± 36.0 (n = 7) on day 1 and falling to 24.5% ± 0.71 (n = 2) by day 10 (Fig. 7D). Overall, hybrid hydrogels exhibit larger burst release and greater variability influenced by drug characteristics, as compared to the slower, more consistent release profiles of synthetic systems.

When comparing the number of hydrogels that continued releasing drug at successive timepoints, synthetic systems consistently outperformed hybrid formulations. By day 5, the number of hybrid hydrogels still releasing drug had dropped by 65% (from 17 to 6), whereas synthetic hydrogels decreased by just 3% (from 34 to 33). This gap widened further over time: at day 30, nearly 95% of hybrid hydrogels had ceased drug release (falling to only 1), while a reduction of only ~35% was observed for synthetic hydrogels with 22 formulations still releasing drug (Fig. 9A). While these trends are dependent on multiple variables and cannot be generalized to polymer class alone, this analysis indicates that synthetic hydrogels are consistently able to sustain drug release for longer durations than hybrid formulations.

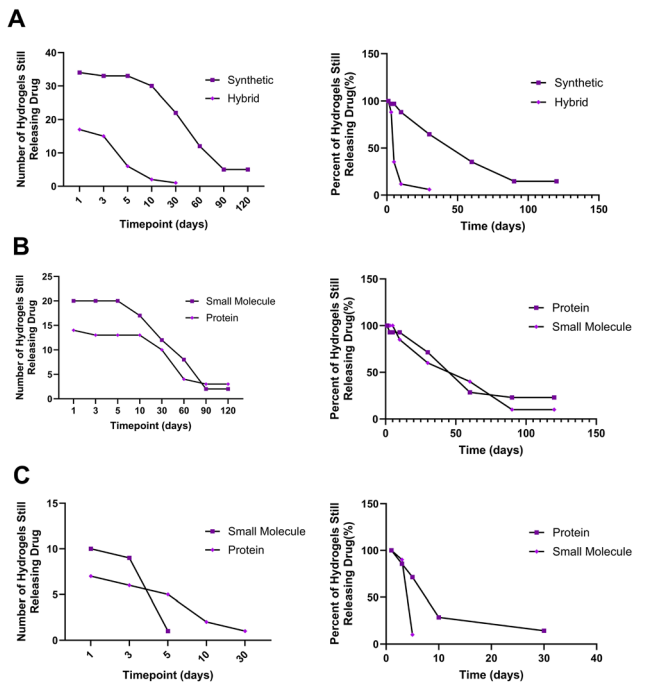

Fig. 9 Number of hydrogels still releasing drug at different timepoints represented as a total number (left) and percent of total (right). Separated by: (A) polymer class; (B) therapeutic class for synthetic hydrogels; (C) therapeutic class for hybrid hydrogels.

Within synthetic hydrogels, no notable differences were observed between small molecules and protein therapeutics, as both subclasses maintained comparable release capacity across timepoints (Fig. 9B). In contrast, release behavior in hybrid systems varied by therapeutic class: small molecule-loaded hybrids declined rapidly, with no release extending beyond day 5, whereas protein-loaded hybrids sustained drug release up to 30 days (Fig. 9C). These results highlight that drug release from synthetic hydrogels is inherently more robust, maintaining prolonged release across diverse formulation ratios and therapeutic types.

Additional formulation considerations

As demonstrated in the present review, polymer selection substantially influences hydrogel performance. However, the formulation process is multifactorial, and hydrogel behavior cannot be fully explained by polymer composition alone. Factors including the method of hydrogel preparation, crosslinking density, and drug-loading approach also play decisive roles in determining mechanical strength, safety, and release kinetics. Although these parameters were not directly assessed in the current analysis, they represent critical design considerations that warrant further discussion, as outlined below.

Method of hydrogel preparation. Hydrogel networks consist of polymer chains interconnected by crosslinks, which may be physical (non-covalent) or chemical (covalent) in nature. These crosslinks are critical for maintaining the three-dimensional, water-swollen structure of the hydrogel, and the method of preparation determines the type of crosslinking achieved. Physical crosslinks arise from electrostatic interactions, hydrogen bonding, and hydrophobic forces. These interactions are reversible, less stable, and tend to degrade more readily under physiological conditions. In contrast, chemical crosslinks involve covalent bonding between polymer chains, formed either through the use of a chemical crosslinker or through reactive functional groups present on the polymer backbone. Chemical crosslinks confer greater structural stability and mechanical strength but may pose a higher risk of adverse biological reactions due to additional chemical moieties.[7,14,76,77]

Chemically crosslinked hydrogels are typically produced through chain-growth polymerization, addition or condensation polymerization, or by radiation methods such as gamma or electron beam polymerization. In contrast, physically crosslinked hydrogels are formed through non-covalent interactions, including ionic interactions, crystallization, stereocomplex formation, hydrophobic interactions (*e.g.*, with hydrophobized polysaccharides), protein interactions, and hydrogen bonding.[77] The type and degree of crosslinking significantly influence the physicochemical and mechanical properties of hydrogels, so the selection of the crosslinking method should be carefully tailored to the characteristics of the polymer and the desired properties of the final formulation. Beyond the type of crosslink, crosslinking density also plays a crucial role in determining hydrogel properties. By modulating the type and degree of crosslinking, key character-

istics such as rigidity, mechanical strength, drug release kinetics, and degradation rate can be controlled.[7,77]

Mechanism of drug entrapment. Drugs can be incorporated into hydrogel matrices either during hydrogel formation or after the matrix has been established. Loading the drug during hydrogel synthesis often results in higher drug loading efficiency but typically requires the drug to be covalently bonded to the polymer chains. In such cases, drug release occurs only after polymer degradation or upon application of an external stimulus to cleave the covalent bonds. When the drug is loaded after hydrogel formation, it interacts with the polymer network primarily through electrostatic or hydrophobic interactions. Electrostatic interactions arise between oppositely charged drug and polymer molecules and can vary in strength. Hydrophobic interactions, which are generally weaker, occur when lipophilic drugs are introduced into the hydrophilic hydrogel matrix. These weaker interactions may lead to reduced stability and less predictable drug release profiles.[9,14]

Mechanism of drug release. Drug release from hydrogels can be governed by diffusion, swelling, or chemical mechanisms. In diffusion-controlled release, drug transport occurs along a concentration gradient. This can be achieved using either a reservoir system (where release is solely diffusion-based) or a matrix system (where both diffusion and polymer degradation contribute to release). In swelling-controlled release, the hydrogel absorbs water, leading to an increase in mesh size that facilitates outward diffusion of drug molecules. If the drug is larger than the initial mesh size, it will only be released upon hydrogel swelling or degradation. Chemically controlled release requires the cleavage of polymer chains or disruption of polymer–drug interactions for drug release. Overall, drug release kinetics depend on multiple factors, including the molecular size of the drug, the strength of polymer–drug interactions, polymer concentration, degradation rate, and the degree of crosslinking within the hydrogel network.[9,14]

Practical challenges in formulation design

In situ forming hydrogels characteristically exhibit an initial burst release immediately following intravitreal injection. This effect arises from unencapsulated or surface-associated drug that diffuses from the matrix prior to complete gelation within the vitreous. The magnitude of burst release is influenced by gelation kinetics as well as drug and polymer physicochemical properties that govern drug distribution within the scaffold.[78] Excessive burst release may result in transient drug concentrations outside the therapeutic window and shorten the intended duration of release.[79] Accordingly, minimizing burst release remains a primary design challenge. Strategies to mitigate this effect include optimizing polymer composition and molecular weight, tuning drug size and hydrophobicity, and employing approaches such as micronization or improved drug–polymer interactions.[78]

Injection volume represents another critical parameter in hydrogel formulation design. Although the mean injection volume reported across the included studies aligns with standard clinical intravitreal injections, the values reported in the literature range widely from 1 μL to 500 μL. Several studies have shown that intraocular pressure (IOP) increases proportionally with the injected volume, with exponential increases observed when volumes exceed 100 μL.[74,80] Because elevated IOP can induce mechanical stress and restrict retinal blood flow, differences in injection volume may significantly influence both safety outcomes and intraocular fluid dynamics.[81] In addition, injection volume can affect depot formation and drug-release behavior. Larger injected volumes may form larger, more interconnected hydrogel networks within the vitreous, which can reduce initial burst release as the drug must diffuse through a greater polymer matrix prior to release. In contrast, smaller injection volumes present a higher surface-area-to-volume ratio between the gel and vitreous, potentially increasing burst release. However, the ultimate structure of the depot formed in the vitreous depends on multiple formulation and procedural variables, including gelation kinetics, injection speed, and polymer composition, in addition to the injected volume. Adherence to a standardized injection volume, such as the 50 μL commonly used in clinical intravitreal injections, would enable objective comparisons moving forward.

Precise control of the lower critical solution temperature (LCST) is also essential. Premature gelation can occur if the formulation transitions within the needle, leading to administration complications. Ideally, the LCST should be at or slightly above room temperature, with reproducible gelation behavior and a gelation time sufficient to permit safe administration. Environmental conditions, particularly elevated ambient temperatures, may also influence performance and should be considered during formulation design. Finally, injectability is governed by solution viscosity prior to gelation.[82] Increased polymer or drug concentrations can elevate viscosity and injection force, potentially limiting administration through small-gauge needles. Therefore, injectability testing is critical for each formulation to ensure clinical feasibility. Notably, nearly all included formulations were described as compatible with intravitreal injection through standard small-gauge needles, suggesting that injectability itself is unlikely to represent a primary barrier to clinical translation.

Gaps in preclinical testing

Although most hydrogel systems are designed to degrade into non-toxic byproducts, few studies comprehensively evaluate degradation behavior. When degradation testing is performed, it is often not conducted to completion, leaving uncertainty regarding long-term material persistence and byproduct safety within the ocular environment. Expanded, time-resolved degradation studies are essential to confirm that breakdown products remain non-toxic and non-inflammatory throughout the full intraocular residence period.

Similarly, limited data directly address the impact of hydrogel swelling and *in situ* gelation on ocular physiology. Excessive swelling could theoretically alter IOP, particularly for *in situ* – forming systems that undergo phase transition within the vitreous. Although existing animal studies generally report favorable safety, standardized guidelines defining acceptable

swelling thresholds for intraocular materials are lacking. As emphasized previously, caution should be exercised when comparing swelling ratio values across studies, as substantial variation in experimental methodologies and calculation approaches limits cross-study comparability. Without methodological consistency, it becomes difficult to reliably compare results between research groups, ultimately hindering the establishment of evidence-based safety thresholds for hydrogel swelling in intravitreal applications.

While animal data was not assessed in the current review, prior to clinical translation, formulations must undergo rigorous safety, pharmacokinetic, and efficacy assessments in relevant animal models. These assessments are essential to not only ensure safety but also provide necessary retinal concentrations and clearance rates of therapeutic compounds to ensure accurate dosing for human translation. Rabbits are frequently used due to pharmacokinetic similarities to humans, and *in silico* models have shown promise in predicting intravitreal drug disposition.[83–85] However, most available data derive from healthy models and conventional solution injections rather than sustained-release hydrogels. Broader inclusion of diseased models, long-term pharmacokinetic profiling, and adherence to standardized reporting frameworks such as ARRIVE[86,87] will strengthen translational readiness and improve the predictive value of preclinical hydrogel studies.

Barriers to large-scale manufacturing

Polymer synthesis for many hydrogel systems is often chemically complex and may require multistep reactions, purification processes, and precise control of reaction conditions. These requirements can increase production costs and limit scalability, thereby reducing translational feasibility. Furthermore, most preclinical studies are not conducted under Good Manufacturing Practice (GMP) conditions, raising concerns regarding batch-to-batch consistency, residual reagents, and potential contamination during production or packaging. Although hydrogel platforms offer substantial design flexibility, this tunability also makes them highly sensitive to minor variations in polymer composition, molecular weight, crosslinking density, and processing parameters. Such sensitivity presents challenges for reproducibility and large-scale manufacturing, underscoring the need for standardized production protocols to support clinical translation.

Sterilization further complicates production, as commonly used methods may cause structural changes or polymer degradation, requiring optimization for each formulation.[88] For biologic therapeutics, aseptic processing[89] of both the drug and hydrogel components is often required to preserve activity and prevent contamination. This requirement increases manufacturing complexity, cost, and regulatory burden.

In addition, while many studies evaluate the stability of released therapeutics over the intended release period, long-term stability of the pre-formed hydrogel matrix and the incorporated drug under storage conditions remains insufficiently characterized. Given the relative novelty of many hydrogel systems included in this analysis, further investigation into scalable manufacturing, sterilization compatibility, and shelf-life stability will be essential to support clinical translation.

Future directions

Currently, only a single intravitreally administered hydrogel has advanced to clinical evaluation. Developed by Ocular

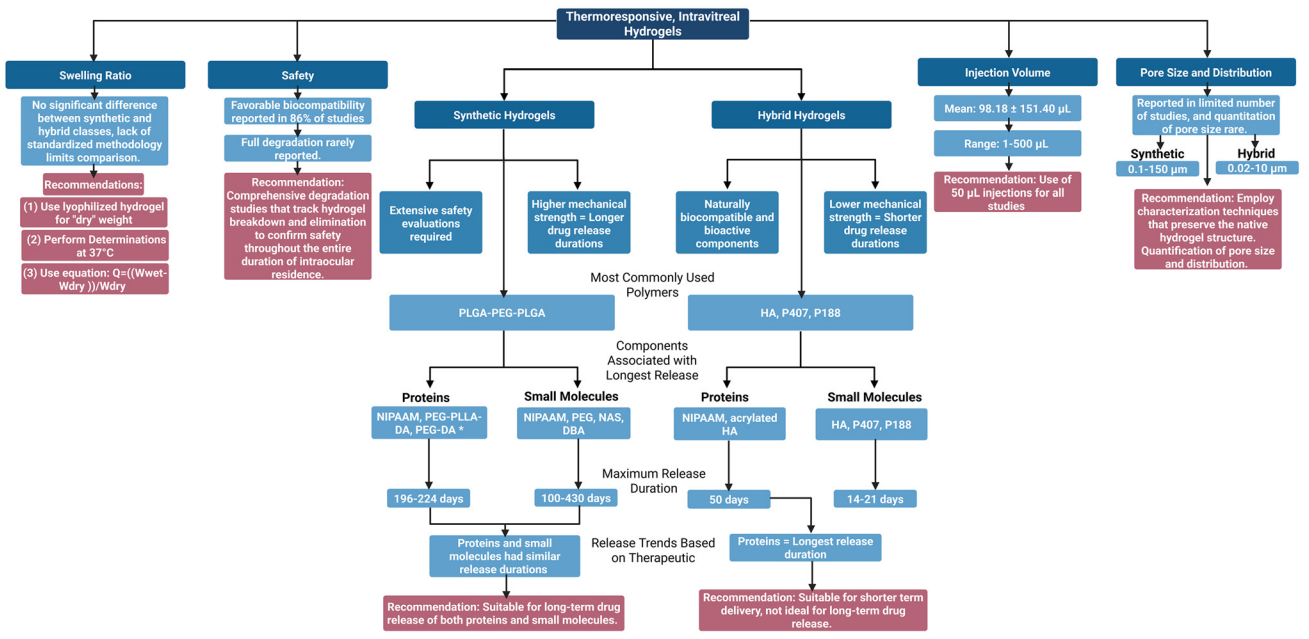

Fig. 10 Summary of key outcomes, drug release trends, and future recommendations. Created in BioRender. Beathard, A. (2026) https://BioRender.com/9muca1j.

Therapeutix, AXPAXLI™ (OTX-TKI) is a PEG-based hydrogel fiber containing microcrystals of axitinib, a tyrosine kinase inhibitor.[90,91] This formulation is designed to provide sustained drug release for up to 9–12 months and has demonstrated promising results in clinical trials.[92,93] In comparison with the formulations evaluated in the present study, only four systems achieved release durations within the 6–14 month range, highlighting the need for intentional and collaborative design frameworks to optimize drug-release profiles and achieve meaningful clinical benefit.

Notably, AXPAXLI™ is an implantable system rather than a thermoresponsive hydrogel. Since thermoresponsive systems undergo a sol–to-gel transition within the vitreous following injection, they enable minimally invasive administration that may improve patient comfort and reduce complications compared with implatable products. Additionally, AXPAXLI™ is administered using a single-use applicator with a 25-gauge needle, whereas many thermosensitive hydrogel systems are designed for injection through finer needles (27–30G), which may further reduce procedural invasiveness. Preliminary safety reports from clinical trials of AXPAXLI™ indicate a higher frequency of ocular adverse events compared with standard aflibercept injections.[94] Therefore, while this system represents an important advancement, the development of formulations that allow simple and safe injection procedures remains an important objective for the field.

The limited clinical progression of these thermoresponsive systems likely reflects both the novelty and heterogeneity of the field. Current preclinical formulations span diverse polymer chemistries, block arrangements, therapeutic payloads, and gelation mechanisms, with substantial variability in experimental design and outcome reporting. The absence of standardized formulation, characterization, and safety-testing frameworks complicates cross-study comparison and slows the identification of reproducible, clinically viable candidates. Fig. 10 summarizes key findings from the included studies and highlights recommended characterization strategies and formulation considerations to guide future development.

As the field matures, the establishment of consensus guidelines for material characterization, degradation assessment, pharmacokinetic evaluation, and ocular safety testing will be critical. Greater methodological standardization, combined with scalable manufacturing strategies and clearly defined regulatory pathways, will be essential to bridge the gap between promising preclinical data and successful clinical translation of thermoresponsive intravitreal hydrogel systems.

Conclusions

Injectable, thermoresponsive hydrogels represent a promising class of biomaterials capable of transforming the management of chronic retinal diseases. Their rational design, however, requires deliberate integration of polymer selection, therapeutic compatibility, and crosslinking chemistry to balance mechanical integrity, water content, and microarchitecture. Establishing this balance is essential to sustain controlled drug release while maintaining long-term biocompatibility. These findings from a systematic review and quantitative analyses synthesize current preclinical data to inform a data-driven, design-oriented framework for developing long-acting hydrogels for intravitreal administration.

Collectively, the reported data emphasize polymer components as dominant determinants of release performance, with synthetic systems offering the most reliable basis for long-acting intravitreal therapies (Fig. 10). All evaluated formulations demonstrated favorable safety and biocompatibility, with no reports of cytotoxicity or adverse ocular effects. Nonetheless, critical knowledge gaps persist, particularly regarding long-term degradation and complete material clearance. Similarly, inconsistent reporting of swelling behavior, pore architecture, and imaging methodologies limited cross-study comparability. Future progress in this field will depend on establishing standardized testing protocols and shared data frameworks to enable meaningful inter-laboratory comparison.

Author contributions

Alexa K. Beathard-Wojan performed data curation, analysis, investigation, methodology, software usage, validation, visualization, and initial manuscript drafting. Dr Vibhuti Agrahari supervised the project, acquired funding, and performed manuscript revisions. All authors were involved in project conceptualization and approved the final manuscript.

Conflicts of interest

There are no conflicts to declare.

Acronyms

Polymers:

AAm	Acrylamide
BOX	2,2-Bis (2-oxazoline)
DA	Diacrylate
DBA	(*r*)-α-Acryloyloxy-β,β-dimethyl-γ-butyrolactone
D-Glu	D-(+)-Glucosamine hydrochloride
HA	Hyaluronan/hyaluronic acid
HA-CHO	Hyaluronan-aldehyde
HA-SH	Thiolated-hyaluronan
HA-Tyr	Tyramine-substituted hyaluronan
HEA	2-Hydroxyethyl acrylate
HEMA	2-Hydroxylethyl methacrylate
HPMC K15M	Hydroxypropyl methylcellulose
MAA	Methacrylic acid
MC	Methylcellulose
mPEG	Methoxy-poly (ethylene glycol)
NAS	*N*-Cryloxysuccinimide

NIPAAM	*N*-Isopropylacrylamide
P188	Poloxamer 188 (Pluronic F-68)
P407	Poloxamer 407 (Pluronic F-127)
PBLA	Poly-(*b*-butyrolactone-*co*-lactic acid)
PCL	Poly(ε-caprolactone)
PEG	Poly(ethylene glycol)
PEOz	Poly(2-ethyl-2-oxazoline)
PLGA	Poly(lactic-*co*-glycolic acid)
PLLA	Poly(L-lactic acid)
PPG	Polypropylene glycol
PSHU	Poly(serinol hexamethylene urea)
PTMC	Poly(trimethylene carbonate)
SA	Succinic anhydride

Assays:

CCK-8	Cell counting kit-8
MTT	3-[4,5-Dimethylthiazol-2-yl]-2,5-diphenyl tetrazolium bromide
MTS	(3-(4,5-Dimethylthiazol-2-yl)-5-(3-carboxymethoxyphenyl)-2-(4-sulfophenyl)-2*H*-tetrazolium, inner salt)
LDH	Lactate dehydrogenase
ELISA	Enzyme-linked immunosorbent assay
SRB	Sulforhodamine B
HET-CAM	Hen's egg test–chorioallantoic membrane

Cell lines:

ARPE	Adult retinal pigment epithelial
RPE	Retinal pigment epithelial
RGC	Retinal ganglion cell
HUVEC	Human umbilical vein endothelial cells

Others:

PRISMA	Preferred reporting items for systematic reviews and meta-analyses
PICOS	Population, intervention, comparison, and outcome
DR	Diabetic retinopathy
AMD	Age-related macular degeneration
wAMD	wet AMD
CNV	Choroidal neovascularization
TNF-α	Tumor necrosis factor-alpha
VEGF	Vascular endothelial growth factor
SEM	Scanning electron microscopy
TEM	Transmission electron microscopy

Data availability

The data supporting this article have been included as part of the supplementary information (SI). Supplementary information: risk of bias descriptors, sensitivity analysis, and descriptors for formulations included in percent release analysis. See DOI: https://doi.org/10.1039/d6bm00104a.

Acknowledgements

Figures were created using BioRender.com, with appropriate attribution provided in the corresponding figure legends. All graphs were generated using GraphPad Prism. During the preparation of this manuscript, the authors used generative AI tools solely for minor editorial purposes, including language refinement and word choice. All scientific content, interpretations, and intellectual contributions are exclusively those of the authors. This research was supported by the University of Oklahoma College of Pharmacy.

References

1 World Health Organization. Vision impairment and blindness. [cited 2025 May 16]. Available from: https://www.who.int/news-room/fact-sheets/detail/blindness-and-visual-impairment.
2 *Ocular Drug Delivery: Advances, Challenges and Applications*, ed. R. T. Addo, Springer International Publishing, Cham, 2016, [cited 2025 May 19]. Available from: https://link.springer.com/10.1007/978-3-319-47691-9, DOI: 10.1007/978-3-319-47691-9.
3 CDC, Vision and Eye Health. 2024, [cited 2025 May 16]. About Common Eye Disorders and Diseases. Available from: https://www.cdc.gov/vision-health/about-eye-disorders/index.html.
4 B. C. Ilochonwu, A. Urtti, W. E. Hennink and T. Vermonden, Intravitreal hydrogels for sustained release of therapeutic proteins, *J. Controlled Release*, 2020, **326**, 419–441, DOI: 10.1016/j.jconrel.2020.07.031, PubMed PMID: 32717302.
5 R. L. Avery, Retina Today. Bryn Mawr Communications; [cited 2025 Sep 17]. CHIEF MEDICAL EDITOR'S PAGE: Reducing the Burden of Intravitreal Injections. Available from: https://retinatoday.com/articles/2011-mar/chief-medical-editors-page-reducing-the-burden-of-intravitreal-injections.
6 E. M. Ahmed, Hydrogel: Preparation, characterization, and applications: A review, *J. Adv. Res.*, 2015, **6**(2), 105–121, DOI: 10.1016/j.jare.2013.07.006.
7 S. Bashir, M. Hina, J. Iqbal, A. H. Rajpar, M. A. Mujtaba, N. A. Alghamdi, *et al.*, Fundamental Concepts of Hydrogels: Synthesis, Properties, and Their Applications, *Polymers*, 2020, **12**(11), 2702, DOI: 10.3390/polym12112702, PubMed PMID: 33207715; PubMed Central PMCID: PMC7697203.
8 H. M. El-Husseiny, E. A. Mady, L. Hamabe, A. Abugomaa, K. Shimada, T. Yoshida, *et al.*, Smart/stimuli-responsive hydrogels: Cutting-edge platforms for tissue engineering and other biomedical applications, *Mater. Today. Bio*, 2021, **13**, 100186, DOI: 10.1016/j.mtbio.2021.100186, PubMed PMID: 34917924; PubMed Central PMCID: PMC8669385.
9 X. Hu, C. Zhang, Y. Xiong, S. Ma, C. Sun and W. Xu, A review of recent advances in drug loading, mathematical

modeling and applications of hydrogel drug delivery systems, *J. Mater. Sci.*, 2024, **59**(32), 15077–15116, DOI: 10.1007/s10853-024-10103-x.

10 K. Y. Wu, D. Akbar, M. Giunta, A. Kalevar and S. D. Tran, Hydrogels in Ophthalmology: Novel Strategies for Overcoming Therapeutic Challenges, *Materials*, 2024, **17**(1), 1, DOI: 10.3390/ma17010086.

11 D. Truong, K. Y. Wu, L. Nguyen and S. D. Tran, Advancements in hydrogel technology for ocular drug delivery, *Explor. BioMat-X*, 2024, **1**(6), 6, DOI: 10.37349/ebmx.2024.00023.

12 Ocular Therapeutix, Inc., A Phase 1 Open-Label, Dose Escalation Study of OTX-TKI for Intravitreal Use in Subjects With Neovascular Age-Related Macular Degeneration (AMD) [Clinical trial registration]. clinicaltrials.gov; 2024, [cited 2025 May 19]. Report No.: NCT03630315. Available from: https://clinicaltrials.gov/study/NCT03630315.

13 A. A. Moshfeghi, A. M. Khanani, D. A. Eichenbaum, C. C. Wykoff, S. Couvillion, S. Xavier, *et al.*, U.S. Phase 1 Study of Intravitreal Axitinib Implant (OTX-TKI) for Neovascular Age-related Macular Degeneration, *Invest. Ophthalmol. Visual Sci.*, 2023, **64**(8), 936.

14 C. Umeyor, E. Uronnachi, P. Kakade, C. Umeyor, E. Uronnachi and P. Kakade, *Hydrogels and Nanogels - Applications in Medicine*. 2024, [cited 2025 May 22]. Available from: https://www.intechopen.com/books/1002608, DOI: 10.5772/intechopen.1000374.

15 I. P. Kaur and S. Kakkar, Nanotherapy for posterior eye diseases, *J. Controlled Release*, 2014, **193**, 100–112, DOI: 10.1016/j.jconrel.2014.05.031.

16 E. Ramsay, T. Lajunen, M. Bhattacharya, M. Reinisalo, K. Rilla, H. Kidron, *et al.*, Selective drug delivery to the retinal cells: Biological barriers and avenues, *J. Controlled Release*, 2023, **361**, 1–19, DOI: 10.1016/j.jconrel.2023.07.028.

17 J. L. Bourges, S. E. Gautier, F. Delie, R. A. Bejjani, J. C. Jeanny, R. Gurny, *et al.*, Ocular Drug Delivery Targeting the Retina and Retinal Pigment Epithelium Using Polylactide Nanoparticles, *Invest. Ophthalmol. Visual Sci.*, 2003, **44**(8), 3562–3569, DOI: 10.1167/iovs.02-1068.

18 P. Mehta, M. Sharma and M. Devi, Hydrogels: An overview of its classifications, properties, and applications, *J. Mech. Behav. Biomed. Mater.*, 2023, **147**, 106145, DOI: 10.1016/j.jmbbm.2023.106145.

19 B. Ahmed, S. Jaiswal, S. Naryal, R. M. Shah, R. G. Alany and I. P. Kaur, In situ gelling systems for ocular drug delivery, *J. Controlled Release*, 2024, **371**, 67–84, DOI: 10.1016/j.jconrel.2024.05.031, PubMed PMID: 38768662.

20 R. Bisht, S. Nirmal, R. Agrawal, G. K. Jain and J. Nirmal, Injectable *in situ* gel depot system for targeted delivery of biologics to the retina, *J. Drug Target.*, 2021, **29**(1), 46–59, DOI: 10.1080/1061186X.2020.1803886, PubMed PMID: 32729731.

21 G. Sha, J. Liu, Z. Jiang, M. Zhu, Y. Zhu, C. Gu, *et al.*, In situ gels: The next new frontier in ophthalmic drug delivery system, *Polym. Adv. Technol.*, 2023, **34**(8), 2646–2662, DOI: 10.1002/pat.6079.

22 A. Garg, R. Agrawal, C. Singh Chauhan and R. Deshmukh, *In situ* gel: A smart carrier for drug delivery, *Int. J. Pharm.*, 2024, **652**, 123819, DOI: 10.1016/j.ijpharm.2024.123819.

23 A. Patel, K. Cholkar, V. Agrahari and A. K. Mitra, Ocular drug delivery systems: An overview, *World J. Pharmacol.*, 2013, **2**(2), 47–64, DOI: 10.5497/wjp.v2.i2.47, PubMed PMID: 25590022; PubMed Central PMCID: PMC4289909.

24 G. Bonacucina, M. Cespi, G. Mencarelli, G. Giorgioni and G.F. Palmieri, Thermosensitive Self-Assembling Block Copolymers as Drug Delivery Systems, *Polymers*, 2011, **3**(2), 779–811, https://doi.org/10.3390/polym3020779.

25 S. Pardeshi, F. Damiri, M. Zehravi, R. Joshi, H. Kapare, M. K. Prajapati, *et al.*, Functional Thermoresponsive Hydrogel Molecule to Material Design for Biomedical Applications, *Polymers*, 2022, **14**(15), 3126, DOI: 10.3390/polym14153126, PubMed PMID: 35956641; PubMed Central PMCID: PMC9371082.

26 P. A. Janmey and M. Schliwa, Rheology, *Curr. Biol.*, 2008, **18**(15), R639–R641, DOI: 10.1016/j.cub.2008.05.001, PubMed PMID: 18682198; PubMed Central PMCID: PMC2895991.

27 H. Omidian and K. Park, Introduction to Hydrogels, in *In: Biomedical Applications of Hydrogels Handbook*, Springer, New York, NY, 2010, pp. 1–16, [cited 2025 May 24]. Available from: https://link.springer.com/chapter/10.1007/978-1-4419-5919-5_1, DOI: 10.1007/978-1-4419-5919-5_1.

28 R. Wang, C. Cheng, H. Wang and D. Wang, Swollen hydrogel nanotechnology: Advanced applications of the rudimentary swelling properties of hydrogels, *ChemPhysMater*, 2024, **3**(4), 357–375, DOI: 10.1016/j.chphma.2024.07.006.

29 K. Wang and Z. Han, Injectable hydrogels for ophthalmic applications, *J. Controlled Release*, 2017, **268**, 212–224, DOI: 10.1016/j.jconrel.2017.10.031, PubMed PMID: 29061512; PubMed Central PMCID: PMC5722685.

30 C. C. Lin and A. T. Metters, Hydrogels in controlled release formulations: network design and mathematical modeling, *Adv. Drug Delivery Rev.*, 2006, **58**(12–13), 1379–1408, DOI: 10.1016/j.addr.2006.09.004, PubMed PMID: 17081649.

31 L. García, M. R. Aguilar and J. S. Román, Biodegradable Hydrogels for Controlled Drug Release, in *Biomedical Applications of Hydrogels Handbook*, Springer, New York, NY, 2010, pp. 147–155, [cited 2025 May 26]. Available from: https://link.springer.com/chapter/10.1007/978-1-4419-5919-5_8, DOI: 10.1007/978-1-4419-5919-5_8.

32 Covidence, [cited 2025 Dec 3]. Covidence - Better systematic review management. Available from: https://www.covidence.org/.

33 J. P. Higgins, J. Savović, M. J. Page, R. G. Elbers, and J. A. C. Sterne, Chapter 8: Assessing risk of bias in a randomized trial, in *Cochrane Handbook for Systematic Reviews of Interventions version 6.5*, 2024. Available from cochrane.org/handbook.

34 J. A. C. Sterne, Risk of bias tools – RoB 2 tool. [cited 2025 Sep 12]. Available from: https://www.riskofbias.info/welcome/rob-2-0-tool.

35 AMETEK Brookfield, More Solutions to Sticky Problems. [cited 2025 Nov 12]. Available from: https://www.powder-

bulksolids.com/instrumentation-control/solutions-to-sticky-problems.

36 M. Kim, M. Y. Jung, D. Y. Lee, S. M. Ahn, G. M. Lee and C. Y. Park, How to Fabricate Hyaluronic Acid for Ocular Drug Delivery, *Pharmaceutics*, 2024, **16**(12), 1604, DOI: 10.3390/pharmaceutics16121604, PubMed PMID: 39771582; PubMed Central PMCID: PMC11680071.

37 B. C. Ilochonwu, S. A. van der Lugt, A. Annala, G. Di Marco, T. Sampon, J. Siepmann, *et al.*, Thermo-responsive Diels-Alder stabilized hydrogels for ocular drug delivery of a corticosteroid and an anti-VEGF fab fragment, *J. Controlled Release*, 2023, **361**, 334–349, DOI: 10.1016/j.jconrel.2023.07.052.

38 L. Wang, Y. Jiang, Y. Yao, Y. Deng, Z. Liu, J. Ding, *et al.*, Injectable drug-loaded thermosensitive hydrogel delivery system for protecting retina ganglion cells in traumatic optic neuropathy, *Regener. Biomater.*, 2024, **11**, rbae124, DOI: 10.1093/rb/rbae124, PubMed PMID: 39569076; PubMed Central PMCID: PMC11578600.

39 K. M. Rudeen, W. Liu, W. F. Mieler and J. J. Kang-Mieler, Simultaneous Release of Aflibercept and Dexamethasone from an Ocular Drug Delivery System, *Curr. Eye Res.*, 2022, **47**(7), 1034–1042, DOI: 10.1080/02713683.2022.2053166, PubMed PMID: 35343355; PubMed Central PMCID: PMC9906966.

40 S. Awwad, A. Al-Shohani, P. T. Khaw and S. Brocchini, Comparative Study of In Situ Loaded Antibody and PEG-Fab NIPAAM Gels, *Macromol. Biosci.*, 2018, **18**(2), DOI: 10.1002/mabi.201700255, PubMed PMID: 29205853.

41 B. M. Rauck, T. R. Friberg, C. A. Medina Mendez, D. Park, V. Shah, R. A. Bilonick, *et al.*, Biocompatible reverse thermal gel sustains the release of intravitreal bevacizumab in vivo, *Invest. Ophthalmol. Vis. Sci.*, 2014, **55**(1), 469–476, DOI: 10.1167/iovs.13-13120.

42 C. C. Hu, J. R. Chaw, C. F. Chen and H. W. Liu, Controlled release bevacizumab in thermoresponsive hydrogel found to inhibit angiogenesis, *Biomed. Mater. Eng.*, 2014, **24**(6), 1941–1950, DOI: 10.3233/BME-141003.

43 W. Liu, B. S. Lee, W. F. Mieler and J. J. Kang-Mieler, Biodegradable Microsphere-Hydrogel Ocular Drug Delivery System for Controlled and Extended Release of Bioactive Aflibercept In Vitro, *Curr. Eye Res.*, 2019, **44**(3), 264–274, DOI: 10.1080/02713683.2018.1533983, PubMed PMID: 30295090; PubMed Central PMCID: PMC7216294.

44 C. R. Osswald and J. J. Kang-Mieler, Controlled and Extended In Vitro Release of Bioactive Anti-Vascular Endothelial Growth Factors from a Microsphere-Hydrogel Drug Delivery System, *Curr. Eye Res.*, 2016, **41**(9), 1216–1222, DOI: 10.3109/02713683.2015.1101140, PubMed PMID: 26764892.

45 B. Xie, L. Jin, Z. Luo, J. Yu, S. Shi, Z. Zhang, *et al.*, An injectable thermosensitive polymeric hydrogel for sustained release of Avastin® to treat posterior segment disease, *Int. J. Pharm.*, 2015, **490**(1–2), 375–383, DOI: 10.1016/j.ijpharm.2015.05.071.

46 C. H. Wang, Y. S. Hwang, P. R. Chiang, C. R. Shen, W. H. Hong and G. H. Hsiue, Extended release of bevacizumab by thermosensitive biodegradable and biocompatible hydrogel, *Biomacromolecules*, 2012, **13**(1), 40–48, DOI: 10.1021/bm2009558.

47 J. J. Kang Derwent and W. F. Mieler, Thermoresponsive hydrogels as a new ocular drug delivery platform to the posterior segment of the eye, *Trans. Am. Ophthalmol. Soc.*, 2008, **106**, 206–213, PubMed PMID: 19277236; PubMed Central PMCID: PMC2646442.

48 K. Xue, X. Zhao, Z. Zhang, B. Qiu, Q. S. W. Tan, K. H. Ong, *et al.*, Sustained delivery of anti-VEGFs from thermogel depots inhibits angiogenesis without the need for multiple injections, *Biomater. Sci.*, 2019, **7**(11), 4603–4614, DOI: 10.1039/C9BM01049A.

49 S. Patel, R. Vaishya, X. Yang, D. Pal and A. Mitra, Novel Thermosensitive Pentablock Copolymers for Sustained Delivery of Proteins in the Treatment of Posterior Segment Diseases, *Protein Pept. Lett.*, 2014, **21**(11), 1185–1200, DOI: 10.2174/0929866521111410011220 54.

50 L. C. du Toit, Y. E. Choonara and V. Pillay, An Injectable Nano-Enabled Thermogel to Attain Controlled Delivery of p11 Peptide for the Potential Treatment of Ocular Angiogenic Disorders of the Posterior Segment, *Pharmaceutics*, 2021, **13**(2), 176, DOI: 10.3390/pharmaceutics13020176, PubMed PMID: 33525495; PubMed Central PMCID: PMC7910951.

51 G. Prosperi-Porta, B. Muirhead and H. Sheardown, Tunable release of ophthalmic therapeutics from injectable, resorbable, thermoresponsive copolymer scaffolds, *J. Biomed. Mater. Res., Part B*, 2017, **105**(1), 53–62, DOI: 10.1002/jbm.b.33501, PubMed PMID: 26415630.

52 A. Aragón-Navas, J. J. López-Cano, M. A. S Johnson, M. Vicario-de-la-Torre, V. Andrés-Guerrero, *et al.*, Smart biodegradable hydrogels: Drug-delivery platforms for treatment of chronic ophthalmic diseases affecting the back of the eye, *Int. J. Pharm.*, 2024, **649**, 123653, DOI: 10.1016/j.ijpharm.2023.123653.

53 K. Pachis, S. Blazaki, M. Tzatzarakis, P. Klepetsanis, E. Naoumidi, M. Tsilimbaris, *et al.*, Sustained release of intravitreal flurbiprofen from a novel drug-in-liposome-in-hydrogel formulation, *Eur. J. Pharm. Sci.*, 2017, **109**, 324–333, DOI: 10.1016/j.ejps.2017.08.028.

54 A. Annala, B. C. Ilochonwu, D. Wilbie, A. Sadeghi, W. E. Hennink and T. Vermonden, Self-Healing Thermosensitive Hydrogel for Sustained Release of Dexamethasone for Ocular Therapy, *ACS Polym. Au*, 2023, **3**(1), 118–131, DOI: 10.1021/acspolymersau.2c00038.

55 S. Sapino, E. Peira, D. Chirio, G. Chindamo, S. Guglielmo, S. Oliaro-Bosso, *et al.*, Thermosensitive Nanocomposite Hydrogels for Intravitreal Delivery of Cefuroxime, *Nanomaterials*, 2019, **9**(10), 1461, DOI: 10.3390/nano9101461, PubMed PMID: 31618969; PubMed Central PMCID: PMC6835325.

56 J. J. López-Cano, A. Sigen, V. Andrés-Guerrero, H. Tai, I. Bravo-Osuna, I. T. Molina-Martínez, *et al.* Thermo-Responsive PLGA-PEG-PLGA Hydrogels as Novel Injectable Platforms for Neuroprotective Combined Therapies in the

Treatment of Retinal Degenerative Diseases, *Pharmaceutics*, 2021, **13**(2), 234, DOI: 10.3390/pharmaceutics13020234, PubMed PMID: 33562265; PubMed Central PMCID: PMC7915560.

57 M. Zou, R. Jin, Y. Hu, Y. Zhang, H. Wang, G. Liu, *et al.*, A thermo-sensitive, injectable and biodegradable in situ hydrogel as a potential formulation for uveitis treatment, *J. Mater. Chem. B*, 2019, **7**(28), 4402–4412, DOI: 10.1039/C9TB00939F.

58 L. Wang, S. Zhang, Y. Han, S. Tang, J. Li, L. Bu, *et al.*, An effective pharmacological hydrogel induces optic nerve repair and improves visual function, *Sci. China Life Sci.*, 2023, **67**, 529–542, DOI: 10.1007/s11427-023-2394-3.

59 R. Huang, B. Jia, D. Su, M. Li, Z. Xu, C. He, *et al.*, Plant exosomes fused with engineered mesenchymal stem cell-derived nanovesicles for synergistic therapy of autoimmune skin disorders, *J. Extracell. Vesicles*, 2023, **12**(10), e12361, DOI: 10.1002/jev2.12361, PubMed PMID: 37859568; PubMed Central PMCID: PMC10587508.

60 L. Zhang, W. Shen, J. Luan, D. Yang, G. Wei, L. Yu, *et al.*, Sustained intravitreal delivery of dexamethasone using an injectable and biodegradable thermogel, *Acta Biomater.*, 2015, **23**, 271–281, DOI: 10.1016/j.actbio.2015.05.005.

61 A. Famili, M. Y. Kahook and D. Park, A combined micelle and poly(serinol hexamethylene urea)-co-poly(N-isopropylacrylamide) reverse thermal gel as an injectable ocular drug delivery system, *Macromol. Biosci.*, 2014, **14**(12), 1719–1729, DOI: 10.1002/mabi.201400250.

62 Q. Wang, C. Sun, B. Xu, J. Tu and Y. Shen, Synthesis, physicochemical properties and ocular pharmacokinetics of thermosensitive in situ hydrogels for ganciclovir in cytomegalovirus retinitis treatment, *Drug Delivery*, 2018, **25**(1), 59–69, DOI: 10.1080/10717544.2017.1413448.

63 DrugBank|Biopharma Intelligence, [cited 2026 Feb 13]. Available from: https://go.drugbank.com/.

64 X. Jiang, C. Liu, Q. Zhang, Y. Lv, C. Lu, W. Su, *et al.*, Strategic delivery of rapamycin and ranibizumab with intravitreal hydrogel depot disrupts multipathway-driven angiogenesis loop for boosted wAMD therapy, *J. Controlled Release*, 2025, **377**, 239–255, DOI: 10.1016/j.jconrel.2024.11.011, PubMed PMID: 39528095.

65 S. L. Taheri, M. Rezazadeh, F. Hassanzadeh, V. Akbari, A. Dehghani, A. Talebi, *et al.*, Preparation, physicochemical, and retinal anti-angiogenic evaluation of poloxamer hydrogel containing dexamethasone/avastin-loaded chitosan-N-acetyl-L-cysteine nanoparticles, *Int. J. Biol. Macromol.*, 2022, **220**, 1605–1618, DOI: 10.1016/j.ijbiomac.2022.09.101, PubMed PMID: 36116595.

66 S. Awwad, A. Abubakre, U. Angkawinitwong, P. T. Khaw and S. Brocchini, In situ antibody-loaded hydrogel for intravitreal delivery, *Eur. J. Pharm. Sci.*, 2019, **137**, 104993, DOI: 10.1016/j.ejps.2019.104993, PubMed PMID: 31302214.

67 R. Egbu, S. Brocchini, P. T. Khaw and S. Awwad, Antibody loaded collapsible hyaluronic acid hydrogels for intraocular delivery, *Eur. J. Pharm. Biopharm.*, 2018, **124**, 95–103, DOI: 10.1016/j.ejpb.2017.12.019, PubMed PMID: 29294367.

68 E. O. Bakhrushina, A. I. Dubova, M. S. Nikonenko, V. V. Grikh, M. M. Shumkova, T. V. Korochkina, *et al.*, Thermosensitive Intravitreal In Situ Implant of Cefuroxime Based on Poloxamer 407 and Hyaluronic Acid, *Gels*, 2023, **9**(9), 693, DOI: 10.3390/gels9090693.

69 T. Xiong, X. Li, Y. Zhou, Q. Song, R. Zhang, L. Lei, *et al.*, Glycosylation-enhanced biocompatibility of the supramolecular hydrogel of an anti-inflammatory drug for topical suppression of inflammation, *Acta Biomater.*, 2018, **73**, 275–284, DOI: 10.1016/j.actbio.2018.04.019, PubMed PMID: 29660509.

70 C. Liu, W. Su, X. Jiang, Y. Lv, F. Kong, Q. Chen, *et al.*, A Sustainable Retinal Drug Co-Delivery for Boosting Therapeutic Efficacy in wAMD: Unveiling Multifaceted Evidence and Synergistic Mechanisms, *Adv. Healthc. Mater.*, 2024, **13**(14), e2303659, DOI: 10.1002/adhm.202303659.

71 W. Su, C. Liu, X. Jiang, Y. Lv, Q. Chen, J. Shi, *et al.*, An intravitreal-injectable hydrogel depot doped borneol-decorated dual-drug-coloaded microemulsions for long-lasting retina delivery and synergistic therapy of wAMD, *J. Nanobiotechnology*, 2023, **21**(1), 71, DOI: 10.1186/s12951-023-01829-y, PubMed PMID: 36859261; PubMed Central PMCID: PMC9976542.

72 V. Delplace, A. Ortin-Martinez, E. L. S. Tsai, A. N. Amin, V. Wallace and M. S. Shoichet, Controlled release strategy designed for intravitreal protein delivery to the retina, *J. Controlled Release*, 2019, **293**, 10–20, DOI: 10.1016/j.jconrel.2018.11.012, PubMed PMID: 30419267.

73 J. Aigoin, B. Payré, J. M. Moncla, M. Escudero, D. Goudouneche, D. Ferri-Angulo, *et al.*, Comparative Analysis of Electron Microscopy Techniques for Hydrogel Microarchitecture Characterization: SEM, Cryo-SEM, ESEM, and TEM, *ACS Omega*, 2025, **10**(15), 14687–14698, DOI: 10.1021/acsomega.4c08096.

74 L. L. M. Agra, A. Sverstad, T. A. Chagas, R. H. Araújo, L. G. Oliveira, O. Kristianslund, *et al.*, Accuracy, Precision, and Residual Volume of Commonly Used Syringes for Intravitreal Injections and the Impact on Intraocular Pressure, *Ophthalmol. Retina*, 2023, **7**(10), 892–900, DOI: 10.1016/j.oret.2023.06.003, PubMed PMID: 37302655.

75 American Academy of Ophthalmology, 2013, [cited 2025 Aug 18]. How to Give Intravitreal Injections. Available from: https://www.aao.org/eyenet/article/how-to-give-intravitreal-injections.

76 C. R. Lynch, P. P. D. Kondiah, Y. E. Choonara, L. C. du Toit, N. Ally and V. Pillay, Hydrogel Biomaterials for Application in Ocular Drug Delivery, *Front. Bioeng. Biotechnol.*, 2020, **8**, 228, DOI: 10.3389/fbioe.2020.00228. PubMed PMID: 32266248; PubMed Central PMCID: PMC7099765.

77 J. Maitra and V. K. Shukla, Cross-linking in Hydrogels - A Review, *Am. J. Polym. Sci.*, 2014, **4**(2), 25–31, DOI: 10.5923/j.ajps.20140402.01.

78 X. Huang and C. S. Brazel, On the importance and mechanisms of burst release in matrix-controlled drug delivery systems, *J. Controlled Release*, 2001, **73**(2), 121–136, DOI: 10.1016/S0168-3659(01)00248-6.

79 Y. Fu and W. J. Kao, Drug Release Kinetics and Transport Mechanisms of Non-degradable and Degradable Polymeric Delivery Systems, *Expert Opin. Drug Deliv.*, 2010, **7**(4), 429–444, DOI: 10.1517/17425241003602259, PubMed PMID: 20331353; PubMed Central PMCID: PMC2846103.

80 A. Allmendinger, Y. L. Butt and C. Mueller, Intraocular pressure and injection forces during intravitreal injection into enucleated porcine eyes, *Eur. J. Pharm. Biopharm.*, 2021, **166**, 87–93, DOI: 10.1016/j.ejpb.2021.06.001.

81 R. Machiele, M. Motlagh, M. Zeppieri and B. C. Patel, Intraocular Pressure, in *StatPearls*, StatPearls Publishing, Treasure Island (FL), 2025, [cited 2026 Jan 14]. Available from: https://www.ncbi.nlm.nih.gov/books/NBK532237/, PubMed PMID: 30335270.

82 Rheology of Thermosensitive Injectable Polymer Hydrogels. Rheology Lab. [cited 2026 Feb 17]. Available from: https://www.rheologylab.com/articles/pharmaceutical-rheology/rheology-of-thermosensitive-injectable-polymer-hydrogels/.

83 E. M. del Amo and A. Urtti, Rabbit as an animal model for intravitreal pharmacokinetics: Clinical predictability and quality of the published data, *Exp. Eye Res.*, 2015, **137**, 111–124, DOI: 10.1016/j.exer.2015.05.003.

84 A. Sadeghi, A. Subrizi, E. M. Del Amo and A. Urtti, Mathematical Models of Ocular Drug Delivery, *Invest. Ophthalmol. Visual Sci.*, 2024, **65**(11), 28, DOI: 10.1167/iovs.65.11.28, PubMed PMID: 39287588; PubMed Central PMCID: PMC11412384.

85 E. M. del Amo, K. S. Vellonen, H. Kidron and A. Urtti, Intravitreal clearance and volume of distribution of compounds in rabbits: In silico prediction and pharmacokinetic simulations for drug development, *Eur. J. Pharm. Biopharm.*, 2015, **95**(Part B), 215–226, DOI: 10.1016/j.ejpb.2015.01.003.

86 N. Percie du Sert, V. Hurst, A. Ahluwalia, S. Alam, M. T. Avey, M. Baker, *et al.*, The ARRIVE guidelines 2.0: Updated guidelines for reporting animal research*, *J. Cereb. Blood Flow Metab.*, 2020, **40**(9), 1769–1777, DOI: 10.1177/0271678X20943823, PubMed PMID: 32663096; PubMed Central PMCID: PMC7430098.

87 Home|ARRIVE Guidelines, [cited 2026 Jan 26]. Available from: https://arriveguidelines.org/.

88 R. Galante, T. J. A. Pinto, R. Colaço and A. P. Serro, Sterilization of hydrogels for biomedical applications: A review, *J. Biomed. Mater. Res., Part B*, 2018, **106**(6), 2472–2492, DOI: 10.1002/jbm.b.34048, PubMed PMID: 29247599.

89 S. A. C. Bento, M. C. Gaspar, P. Coimbra, H. C. de Sousa and M. E. M. Braga, A review of conventional and emerging technologies for hydrogels sterilization, *Int. J. Pharm.*, 2023, **634**, 122671, DOI: 10.1016/j.ijpharm.2023.122671.

90 AXPAXLITM|Advanced Sustained-Release Treatment for Retinal Diseases. Ocular Therapeutix. [cited 2026 Feb 12]. Available from: https://www.ocutx.com/pipeline/axpaxli/.

91 M. Mahoney, OTX-TKI shows durable results in treatment of neovascular AMD, *Ocular Surgery News*, 2024. Available from: https://www.healio.com/news/ophthalmology/20241011/otxtki-shows-durable-results-in-treatment-of-neovascular-amd.

92 A. Khanani, P. Pecen and R. G. Ozden. Twelve-Month Data From a Phase 1 Clinical Trial of OTX-TKI for Wet AMD. [cited 2026 Mar 13]. Available from: https://digital.retinalphysician.com/publication/frame.php?i=803513&p=&pn=&ver=html5&view=articleBrowser&article_id=4652242.

93 P. Dugel and J. Coletti, Ocular Therapeutix' bold vision to redefine retinal disease treatment, RBCCM, 2025, [cited 2026 Mar 13]. Available from: https://www.rbccm.com/en/insights/2025/07/ocular-therapeutix-bold-vision.

94 D. A. Eichenbaum, 52-week Sustained Efficacy and Treatment Burden Reduction with OTX-TKI in the US Phase 1 Trial for nAMD, *American Academy of Ophthalmology Annual Meeting*, 2024. Available from: https://investors.ocutx.com/static-files/a6148d04-e289-40c0-9b2b-233c22ec0458.